Assessment of hydrogen supply chain for transport sector of Sweden

JOSÉ RODRIGUES

	Master of Science Thesis: **Assessment of hydrogen supply chain for transport sector of Sweden** José Maria Soares Rodrigues	
Approved	Examiner **Prof. Mohammad Reza Hesamzadeh**	Supervisor **Jagruti R. Thakur**
	Industrial Supervisor	Contact Person **Jagruti R. Thakur**

Abstract

Fuel cell electric vehicles, powered by hydrogen are an enticing alternative to fossil-fuel vehicles in order to reduce greenhouse gas emissions and consequently accomplish the environmental targets set to tackle the environmental crisis. It is crucial to develop the appropriate infrastructure if the FCEVs are to be successfully accepted as an alternative to fossil-fuel vehicles.

This study aims to carry out a techno-economic analysis of different hydrogen supply chain designs, that are coupled with the Swedish electricity system in order to study the inter-dependencies between them. The supply chain designs comprehend centralised production, decentralised production and a combination of both. The outputs of the hydrogen supply chain model include the hydrogen refuelling stations' locations, the electrolyser's locations and their respective sizes as well as the operational schedule. Both the hydrogen supply chain designs and the electricity system were parameterized with data for 2030. The supply chain design is modelled to minimize the overall cost while ensuring the hydrogen demands are met. The mixed-integer linear programming problems were modelled using Python and the optimisation software was Gurobi.

The hydrogen models were run for two different scenarios, one that considers seasonal variations in hydrogen demand, and another that does not. The results show that for the scenario with seasonal variation the supply chain costs are higher than for the scenario without seasonal variation, regardless of the supply chain design. In addition, the hydrogen supply chain design with the minimal cost is based on decentralised hydrogen production.

Keywords
Hydrogen, Hydrogen Supply Chain, Elecrolysis, 2030, Sweden, Electricity prices, MILP, Optimization.

Sammanfattning

Bränslecellsdrivna elbilar, som drivs av vätgas, är ett lockande alternativ till fossildrivna fordon för att minska växthusgasutsläppen och därigenom uppnå de miljömål som satts för att tackla miljökrisen. Det är avgörande att utveckla lämplig infrastruktur om FCEV:er ska accepteras som ett alternativ till fossildrivna fordon.

Denna studie syftar till att utföra en teknisk-ekonomisk analys av olika vätgas supply kedjedesign som är kopplade till det svenska elsystemet för att studera beroendeförhållandena mellan dem. Försörjningskedjans design omfattar centraliserad produktion, decentraliserad produktion och en kombination av båda. Resultaten från vätgas supply kedja modellen inkluderar vätgasmackarnas placeringar, elektrolysörernas placeringar och deras respektive storlekar samt den operationella schemat. Både vätgas supplykedjedesi och elsystemet parameteriserades med data för 2030. Supplykedjedesignen modellerades för att minimera de totala kostnaderna samtidigt som vätgasbehoven uppfylls. Mixed-integer lineära programmeringsproblem modellerades med hjälp av Python och optimeringsprogramvaran Gurobi.

Vätgasmodellerna kördes för två olika scenarier, ett som tar hänsyn till säsongsvariationer i vätgasbehovet och ett annat som inte gör det. Resultaten visar att för scenariet med säsongsvariation är supply kedja kostnaderna högre än för scenariot utan säsongsvariation, oavsett supplykedjedesignen. Dessutom är vätgas supply kedjedesignen med minimal kostnad baserad på decentraliserad vätgasproduktion.

Acknowledgements

I would like to start by extending my gratitude to Jagruti, for her role in the successful completion of this thesis. At last, a special thank you to my parents and my friends, who have been a cornerstone in my academic years.

To my parents I must extend the most heartfelt gratitude for their unconditional support throughout every stage of my academic life, being always present and encouraging me to make my decisions, free of fears, knowing they would always be there.

To my fellow colleagues, the ones who started this journey with me in Instituto Superior Técnico, José Ralo, José Luz, Magnus Schneider, Francisco Peres and João Domingues, thank you for sharing with me some great moments, which I will take with me for the rest of my life.

To my amazing group of the Petit Gâteau sessions, José Luz, Inês Mendes Letra, Vasco Maria Marques, Catarina Almeida and Rodrigo Fernandes, thank you for one of the best years, it was truly memorable living in the 45 with you all.

Contents

List of Figures

List of Tables

Nomenclature

$BEVs$ Battery Electric Vehicles

$FCEVs$ Fuel Cell Electric Vehicles

$GH2$ Centralised design in gaseous state

HRS Hydrogen Refuelling Station

$HRSs$ Hydrogen Refuelling Stations

$LH2$ Centralised design in liquid state

PEM Polymer Electrolyte Membrane

RES Renewable Energy Sources

TSO Transmission System Operator

Chapter 1

Introduction

The need to decarbonise today's societies is at a critical tipping point as drought, wildfires, storms, and other natural catastrophes are becoming more frequent and severe worldwide. In order to prevent further climate change, all nations signed the Paris Agreement, which aims to limit global warming to well below 2, preferably to 1.5 degrees Celsius, compared to pre-industrial levels [1]. In addition, the European Green Deal states that every state member must be neutral greenhouse gas emissions by 2050 and reduce net greenhouse gas emissions by at least 55% by 2030 [2].

Due to its ongoing reliance on fossil fuels, in 2019, the transportation sector accounted for 25.8% of total greenhouse gas emissions in the EU. Thus sharing only the stage of the sector with the highest greenhouse gas emissions with the Energy Industries and fuel combustion by users (excl. transport)[3]. In the same year, road transport emitted 72% of all domestic and international transport GHG, thus constituting the highest proportion of overall transport emissions [4]. Therefore, it is a pivotal sector to decarbonise if one is to achieve the targets mentioned above.

In order to fully decarbonise this sector, it is straightforward that vehicles must emit no GHG whatsoever, the so-called zero-emission vehicle (ZEV). Battery electric vehicles (BEV) and hydrogen fuel cell electric vehicles (FCEV) are regarded as the two key technologies to achieve such a carbon-free sector [5]. These innovations are still in their infancy and have not yet made a substantial market impact. Most industry experts predict that the FCEV market will expand in heavier vehicles with high daily use, such as heavy-duty trucks, while the BEV market will develop in lighter vehicles with low daily use. However, each technology presents its own set of unique characteristics, from cost to performance, which results in a set of trade-offs, making it challenging to identify the best decarbonisation approach.

BEVs have been introduced into the market for some years now. However, the high prices, low autonomy and long charging times have been hindering, until now, the penetration of these vehicles. Nevertheless, passenger vehicles are being released with higher and higher autonomies. For instance, in 2022, Mercedes-Benz successfully completed a 1,000 km road trip on a single charge. Some argue that with such a level of autonomy and charging times, BEVs will dominate the market as vehicle purchase prices are also expected to decrease swiftly in the upcoming years and become cheaper than petrol cars by 2027 [6].

Others argue that a multifueled future lies ahead, combining synthetic biofuels, hybrids, batteries, hydrogen fuel cells, etc [7]. These different beliefs can be seen in car manufacturers, for instance, Volkswagen is betting firmly on BEVs due to their higher efficiency compared to FCEVs, whereas Volvo, regarding heavy-duty trucks, is betting on both technologies [8], [9]. BEVs are suitable for urban mobility, local as well as regional distribution applications. However, Volvo believes that for long driving distances, when it's impossible to rely on one's own charging infrastructure, fuel cell technology presents a clear advantage, with longer autonomies and much shorter charging times. Nikola, an American semi-truck manufacturer based in Arizona, states that by 2024 they will be ready to launch a fuel cell semi-truck with charging time up to 20 minutes and autonomy up to approximately 1400 km [10]. However, in order to render both technologies viable, it is crucial to develop appropriate infrastructures [7], [11].

The BEVs' electric network is more mature in its development in comparison to the FCEVs' hydrogen network, and more significantly, it can sustain, to a certain extent, the BEVs now on the road. As of the second quarter of 2021, there are said to be just over 15000 public charging points in Sweden for BEVs, of which 1665 are fast-charging, compared to the mere five hydrogen refuelling stations operational as of July 2022 [12], [13]. There is increasing awareness that switching from existing heavy-duty vehicles to FCEVs powered by hydrogen might help cut transportation emissions globally. Also, it is essential to underline that FCEVs and BEVs should not compete but rather cooperate in developing a zero-emission transportation industry [14].

However, developing such a network is not as straightforward as it may seem, as it originates from a cause-and-effect problem. On the one hand, there should be an assurance that a sufficient number of FCEVs will utilise these stations to justify investment in hydrogen fuelling stations and related infrastructure. On the other hand, customers want assurance that there is an infrastructure to refill their vehicles affordably before they invest in FCEVs. Both public and private organisations are aware of this problem and are looking into potential solutions where the infrastructure is built to support the growth of the FCEV business. Therefore, this study proposes to come up with a hydrogen supply chain design, that depicts the hydrogen demand as accurately as possible and that showcases a potential infrastructure to satisfy that demand.

Chapter 2

Literature Review

This section will describe the recent research conducted for designing a hydrogen supply chain for the transportation sector.

Since hydrogen had already sparked much interest as a potential decarbonisation solution, including for the transportation sector, studies and investments have been conducted on its technology and infrastructure. A UK consultancy firm has ranked Germany as the leading nation in financing a hydrogen economy [15].

Using hydrogen as a transportation fuel requires thoroughly examining the whole supply chain, from production to consumption. Vehicle storage tanks need to be able to store hydrogen without leaking and sustain high pressures. Today, several automakers design their vehicles with compressed hydrogen tanks, which may reach 350 or 700 bars of pressure depending on the kind of vehicle, light duty and heavy duty, respectively [13]. The most economical supply system between manufacturing and transportation has been the subject of several studies. The "state of the art" supply chain is mainly based on pure hydrogen supplied as compressed gas or cryogenic liquid [16], [17].

The study carried out by Yang and Ogden [18] investigates a methodology for evaluating the various transport options for tube or liquid trailer trucks vs pipeline delivery. The study demonstrates that each technology has a very cost-effective specific market and that there is no ideal path for the whole system. Elgowainy and Reddi provide an Excel tool to estimate the price of hydrogen supply while adjusting various input factors, such as FCEV market share, refuelling station capacity, transportation mode, or production output for various delivery scenarios [19]. The study focused on pipeline, tube and liquid trailer as the three primary distribution methods, similar to Yang and Ogden. However, neither model includes a calculation of the hydrogen production cost, it is regarded as

an input instead. As a result, the impact of hydrogen generation on storage demand was not explored. Reuß et al., [20], consider that given the importance of hydrogen mobility as part of a future renewable energy system and the use of electrolysis systems powered by five renewable sources, this impact should not be neglected. Besides, studies [19], [21] have indicated that seasonal storage can play a significant role. However, these studies only comprehended scenarios considering underground solutions, such as salt caverns or abandoned oil fields.

In 2017 high-pressure storage tanks were thought to be cost-intensive (800 $/kg_{H_2} [22]), while the liquefaction of hydrogen was energy intensive (30% of the LHV of hydrogen [23]). As of today, costs for high-pressure tanks have decreased to 600 €/kg_{H_2}, which is a result of the the European project COPERNIC [24]. In addition to the compressed and liquid uses, several other hydrogen storage options are available. The two primary mechanisms for storing hydrogen in addition to conventional compressed and liquid storage are: chemisorption - which uses substances like metal hydrides, chemical hydrides, or liquid organic hydrogen carriers (LOHC); physisorption - which uses substances like carbon nanotubes or metal-organic frameworks (MOF) [25].

Alternative carrier technologies like LOHCs and metal hydrides were considered in the 2010 Nexant Report [26]. This study concluded that "using other carriers in a pathway that releases hydrogen at the fueling station and distributes compressed hydrogen to automobiles will give little or no advantage for fueling station expenses". However, Teichmann [27], [28] demonstrates that the functionality and affordability of storage and transportation are the primary advantages of a LOHC system.

According to Dagdougui [29], most hydrogen supply chain models rely on mathematical optimization techniques to reduce the cost of a specific scenario. However, Reuß et al. considered that there was a lack of modelling approaches that included upcoming technologies like LOHC or supply chains that included seasonal storage. Therefore, Reuß et al. [20] explored the application area of various hydrogen supply chain designs using a point-to-point analysis based on Yang and Ogden's approach, relying on existing data and expanding the investigated technologies. As a result, [20] considers the entire supply chain, from hydrogen production via electrolysis to large-scale storage, to bridge the temporal mismatch between demand and supply, as well as the transportation means and fueling station facilities required to fill a 700 bar compressed gas tank. Furthermore, LOHCs was considered a potential alternate carrier system to evaluate their potential impacts on hydrogen mobility [20].

The following paragraphs are based on a literature review carried out by Reuß et al. [30], and it's based on papers focusing on spatial resolution and often has Germany as a study case. Bolat and Thiel [31], [32]provide an overview of modelling tools for assessing hydrogen infrastructure, distinguishing between analytical and mathematical approaches.

Two distinct application scenarios may be identified after thoroughly analyzing the application of the proposed approaches. Numerous studies have looked into the design of spatially resolved infrastructure for national supply strategies: Seydel [33] employed a GIS-based optimization model, where GIS stands for geographic information system, to develop the cost-optimal hydrogen supply chain for a future FCEV-dominated car market, including hydrogen generation, transportation, and refilling. He developed pipeline and truck transportation for hydrogen distribution. Pipeline routing followed the least expensive pathways regarding territorial characteristics, whereas truck routing followed the German street network. Krieg [34] and Baufumé et al. [35] created a countrywide pipeline system using an iterative network construction method based on a cost-weighted shortest path algorithm. The emphasis, in this case, was on technical feasibility. They looked at two different methods of production: lignite gasification and wind electrolysis. They established seasonal storage as well as a 90-day storage capacity. Robinius et al. [36], [37] investigated a hydrogen supply chain based exclusively on the consumption of surplus electricity using the pipeline algorithm developed by Baufumé et al. [35]. The authors demonstrated that electrolysis from wind energy in northern Germany would be adequate to supply hydrogen to 75% of the German LDV market, with 28 GW of electrolysis capacity operating at 5300 full load hours. In terms of hydrogen storage, they examined a reserve capacity of 60 days that accounted for seasonal changes and a strategic reserve.

Moreno-Benito et al. [38], Almansoori and Betancourt-Torcat [39] and Samsatli [40], modelled and calculated a hydrogen infrastructure for delivering hydrogen to Great Britain's transportation industry by means of mixed-integer linear optimization. As a result, they require a temporal resolution as well as the adoption of storage systems for renewable energy sources' variable power generation. In a case study for Germany, Welder et al. [41] utilized a similar technique. Almansoori and Betancourt-Torcat [39] and Moreno-Benito et al. [38] did not examine storage implementation. Instead, they used a variety of hydrogen production methods. Ochoa Biqué and Zondervan [42] enhanced Almansoori and Betancourt-Torcat [39] analysis by including a complete renewable supply chain. However, the predicted costs were excessively high due to a 2.4 USD/kg calculation mistake in the electrolysis computation.

Yáez et al. [43] proposed a hydrogen supply chain infrastructure based on waste hydrogen, in northern Spain, to reduce fuel costs throughout the transformation to a renewable system. De-Léon Almaraz et al. [44], [45] explored the design of a liquid hydrogen-based supply chain infrastructure in France using a multi-objective optimization that incorporated costs, CO2 emissions, and hazards into the objective function. André et al. [46], [47] studied the deployment of a pipeline network for France in order to reduce pipeline expenses. However, they neglected production, storage and distribution. All of these investigations have one thing in common: the final outcomes are entirely dictated by the production technology. Hydrogen transport is viewed as a means

of balancing subregions rather than gaining deeper insights into the behaviour of transportation technologies or designing a realistic network. Seydel [33] and De Léon Almaraz et al. [44], [45] explore detour factors for truck transport to approximate real routing through streets, whereas Baufumé et al. [35] and Seydel [33] consider pipeline detouring to bypass natural reserves and heavily inhabited regions. Ochoa Biqué and Zondervan [42], as well as Almansoori and Betancourt [39] , evaluate rail transportation without having modelled the rail infrastructure. Almansoori and Betancourt [39] , Ochoa Biqué and Zondervan [42], and Moreno-Benito et al. [38] do not study the distribution of hydrogen within a subregion. Samsatli et al. [40] analyze the distribution and fuelling station costs without taking into account potential fueling station locations.

In addition to research that focuses on a national supply chain configuration in order to create a spatially-resolved network, there are also studies with a technology-focused analysis which are generally independent of regional borders.

The JEC consortium's well-to-wheel assessments [48], [49] investigated several supply chain possibilities for the supply of FCEVs using a broad well-to-tank study, demonstrating that low-emission hydrogen requires renewable energy sources. As mentioned before, Yang and Ogden [22] investigated hydrogen transportation solutions for transmission and distribution, but not across the complete supply chain, from manufacturing to refilling. The Hydrogen Delivery Scenario Analysis Model (HDSAM) [50], as well as The Hydrogen Refueling Station Analysis Model (HRSAM) [51] is part of the H2A model family, which provides a thorough estimate of supply chain costs without geographical resolution. Yang and Ogden [18], as well as the HDSAM [50], divided hydrogen transport into the transmission for long-distance transport and distribution for the "final mile" to the filling station, which was carried out by distinct methods. Furthermore, Teichmann et al. [27], [52] and Moroz et al. [53] assess the costs of technologies, although both are case studies that emphasize a technology without considering the full supply chain. Teichmann et al. [27], [52] emphasized the use of LOHCs, whereas Moroz et al. [53] advocated the use of metal hydrides for hydrogen storage and transport. Wulf et al. [54] performed a life cycle assessment (LCA) of the entire hydrogen supply chain, nonetheless did not examine the system's final cost.

Upon the completion of the literature review, Reuß et al. [30] considered that, overall, the national supply systems seek to build a single cost-effective system. However, most of them lack knowledge about alternate options and competing technologies, as well as technological intricacies. Furthermore, the parameters of the analysis are primarily determined by hydrogen production technology. Technology-focused studies concentrate on the competitiveness of various technologies for a variety of applications and supply chain segments based on a number of assessment criteria, such as CO2 emissions and energy demand. So far, the literature lacks a link between technology-focused and spatially-resolved studies that evaluate various technologies on a national scale.

Reuß et al. proposed in [30] to reduce this gap by examining all aspects of the supply chain, from hydrogen generation to refilling, on a national scale concerning Germany for 2050, taking into account a geographical resolution in terms of prices, primary energy use, and CO2 emissions. Furthermore, to assess the competitiveness of various technologies against one another, a simulation method that provides for a greater level of detail in each phase of the supply chain was chosen over an optimisation. To do this, the model of Reuß et al. [20] is expanded by including spatial resolution in order to portray transportation technologies such as pipelines and trucks.

Scheidt et al. developed a paper [55], which analysis the interdependencies between the production of hydrogen for the transportation sector and the electricity system. In this paper, Scheidt et al. present a model that couples the hydrogen supply chain and electricity system, used to analyse a case study of Germany in 2030. It was concluded that when efficient spatially resolved electricity tariffs are used instead of the current uniform tariffs, electrolyzers are located mainly at low-cost nodes, further away from consumption centres. This resulted in more significant transportation costs for hydrogen but reduced production costs and lower total expenses. Furthermore, congestion management expenses reduced significantly. This paper focused on centralized production, without time-flexible operation and storage capabilities. Moreover, it assumed that electrolysers could only be installed in transmission grid nodes, which was justified as they create large loads and thus require connection to sufficiently large power transformers. The model developed by Scheidt et al. provide a quite significant spatial granularity, at the expense of regarding Germany as an isolated system with no international exchanges of electricity or hydrogen. Therefore, this may affect electricity prices and redispacth costs. In short, the paper describes the model thoroughly, namely the hydrogen supply chain and how it is linked with the electricity system.

Andersson et al. developed a master's thesis [56] in which they evaluated how a potential hydrogen refueling infrastructure, critical for a successful commercialization of FCEVs, may be built in Sweden, as well as the roles and parties that would affect such development. Andersson et al. considered that this new hydrogen value chain would bring several uncertainties, thus, it would be important to understand what roles would be needed and which actors could undertake each role to support the development of a hydrogen refuelling infrastructure. In this study, it was explored qualitatively how would the different actors participate in different scenarios, centralized production dedicated only to supplying the transportation sector, centralized production not only dedicated to this sector, and decentralized production dedicated to supplying FCEVs. For each scenario, Andersson et al. analysed its possibilities and challenges, the value chain, what would be Volvo's role in it and how would the scenario unfold in the long run.

In short, no study was found that investigates a hydrogen supply chain for the transportation sector quantitatively for Sweden. Consequently, this study proposes to

provide a model that represents the hydrogen supply chain for the transportation sector, considering heavy-duty trucks and passenger vehicles, for Sweden in 2030. This study will be based on other works such as [20], [30], [55], however, with adaptations in order to incorporate time-flexible operation and a much higher time resolution. Moreover, it proposes to design a decentralized and mixed model, apart from the centralized one as in the mentioned papers. In this study, seasonal-storage was disregarded as Sweden holds very little potential for any type of underground storage [57], [58] and including tank storage would only increase the complexity of the model and require even more computational specifications. LOHC is regarded as a promising technology, particularly when it is not economically feasible to store hydrogen in large-scale underground facilities [20]. Taking this into consideration, adding that in [55], a LOHC supply chain without storage resulted in the most expensive one, by a very significant margin, LOHC was not included in this study.

Chapter 3

Research objective and questions

The objective of this thesis is to design a potential hydrogen supply chain for the transportation sector coupled with the electricity system, in order to analyse the interdependencies between one another. The outcome of the model will be a proposed system design: where should hydrogen fuel stations be located; where should electrolysers be located and with what sizes; at what time should the electrolysers be operational; which electrolysers supply which hydrogen fuel stations. In addition, the model will also prompt the supply chain's overall cost, in euros per kg_{H_2}, and discriminate it according to its cost components. Such information will be acquired through a techno-economic optimisation, which aims to minimize the overall cost of the supply chain. The aim is also to optimise the electrolysers' location, size and operating hours. Furthermore, the model developed for the hydrogen supply chain shall be reproducible and scalable for other countries and regions.

Research Questions:

- What is the potential demand of hydrogen for heavy-duty trucks and passenger vehicles in Sweden in 2030?

- What are the costs of hydrogen for the transportation sector whilst considering spatial distribution of HRS and hydrogen demand in 2030?

- What are the financial impacts of having this hydrogen demand in the electricity market?

Chapter 4

Methodology

To address the research questions mentioned above, the hydrogen supply chain as well as the electricity system were modelled and then parametrized with data regarding Sweden's transportation sector, namely heavy-duty trucks and passenger vehicles, and Sweden's electricity sector in 2030. As can be seen in figure 4.1, the electricity system was modelled, parametrized and run prior to the hydrogen supply chain models since the hourly electricity prices, in each bidding zone, are used as inputs for the hydrogen production costs. As can be observed in Figure 4.2, the hydrogen supply chain was designed considering centralised production of hydrogen, which is produced via electrolysis, and then transported to hydrogen refuelling stations in both gaseous and liquid states. In contrast, the decentralized supply chain design considers on-site production of hydrogen, which means that each HRS site includes an electrolyser, thus cutting off costs for hydrogen distribution. The mixed design is a combination of centralised and decentralised production. In figure 4.2, it can also be seen that every design was parameterised and modelled for two different scenarios, one which considers seasonal variation and another that does not. The different hydrogen supply chain designs are discussed in Section 4.1.

The centralised and mixed models were modelled aiming to minimize the overall supply chain cost by optimizing the:

- location of electrolysers.

- electrolysers' sizes.

- the operating hours.

11
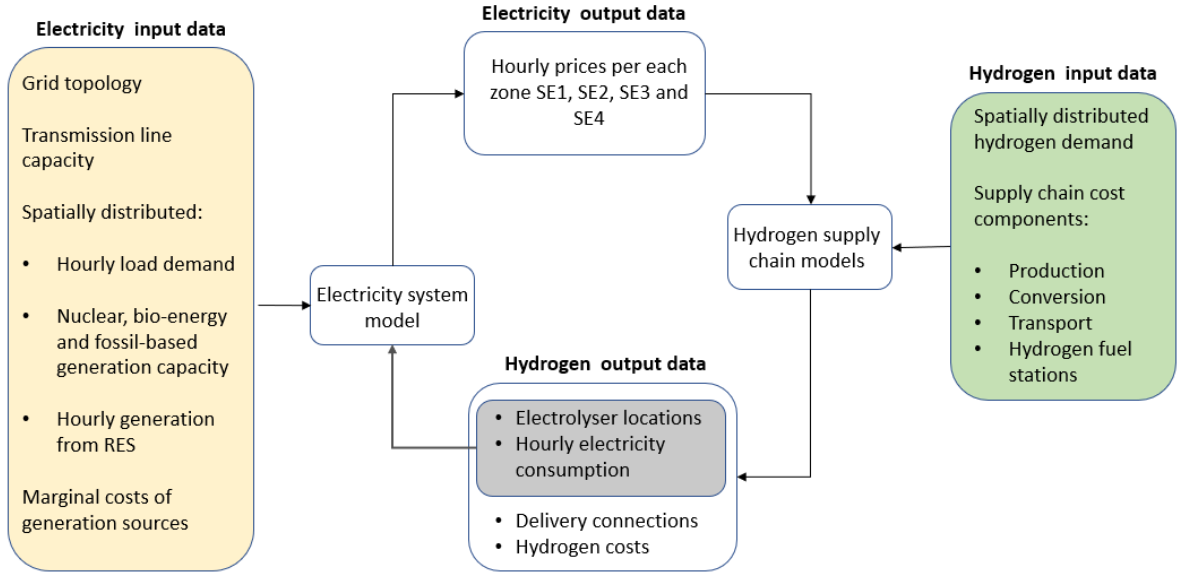
Figure 4.1: Methodology overview: Models for the electricity system and the hydrogen supply chain, soft-linked through inputs and outputs.

The mixed model does not consider the possible conversion of hydrogen from gaseous state to liquid and back as that would increase the model's complexity, particularly in computational requirements. The decentralised model also aimed at minimizing the total supply chain cost, however this time only by optimizing the electrolysers' size and operating hours. This model regards decentralised production which means that hydrogen is produced on the same site as the HRS, therefore there is no optimisation of where electrolysers should be located. Furthermore, since the electrolyser is at the same site as the HRS and directly connected to it, it does not make sense to convert hydrogen from gaseous state to liquid and back, since it is used in gaseous state to power up the FCEVs.

One of the outputs of the hydrogen models is the hourly hydrogen production of every electrolyser, which in fact corresponds to an hourly electricity consumption. Thus, the hourly electricity consumption data is then aggregated according to each bidding zone. In turn, those electricity loads are used as inputs for the electricity system model in order to evaluate the changes in the electricity prices, as can be seen in figure 4.1.

The hydrogen supply chain design is based on the work developed by Scheidt et al., with adaptations to turn the model into a yearly optimisation with an hourly resolution instead of the daily optimisation [55]. Therefore, the model described in sections 4.1 4.2 and 4.3 is more detailed and allows for time-flexible operation, making use of hours with lower prices as well as allowing for variations of the hydrogen demand throughout the

year, bringing the model closer to reality. The work developed by Scheidt et al. was also adapted to design the decentralized as well as the mixed model.
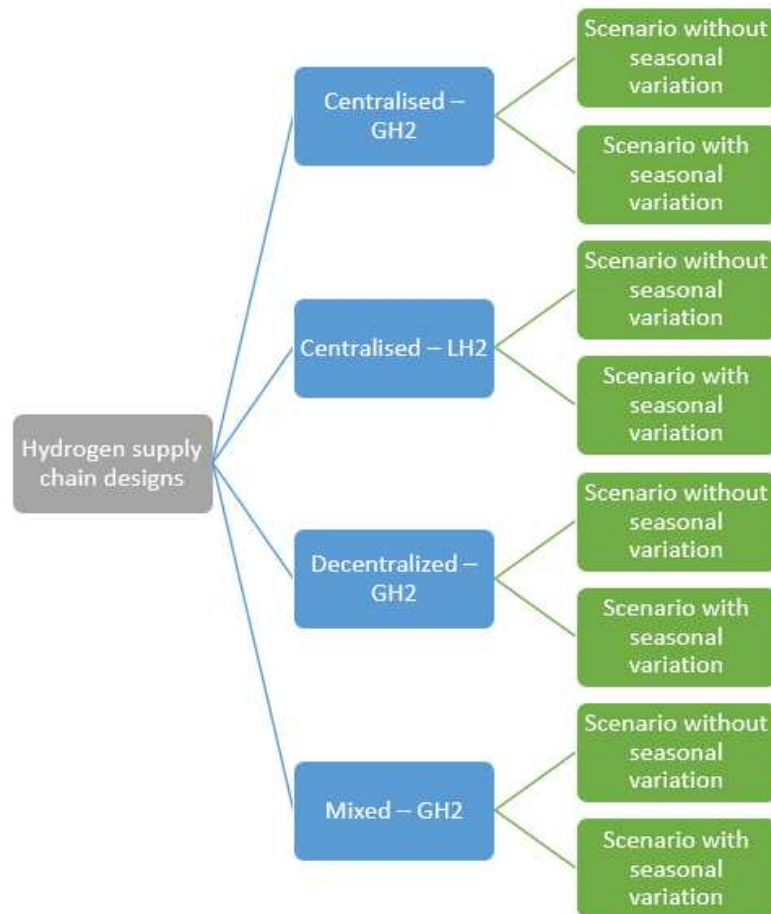
Figure 4.2: Methodology overview: Different hydrogen supply chain designs.

In sections 4.1, 4.2, 4.3, 4.4 and 4.5, different hydrogen supply chain designs and the electricity system model are discussed in detail. In addition, the parameters for the transportation sector and for the electricity system in Sweden in 2030 are described, and the necessary assumptions are explained.

4.1 Centralised hydrogen design - optimisation formulation

The sets and indices applicable for the optimisation model are as follows:

- $p \in P = \{1, 2, ..., 222\}$: Index and set of potential electrolysis power plants.

- $f \in F = \{1, 2, ...99\}$: Index and set of hydrogen fuel stations.

- $t \in T = \{1, 2, ..., 8760\}$: Index and set of hours in a year.

- $d \in D = \{1, 2, ..., 365\}$: Index and set of days in a year.

The decision variables used in the optimisation model are as follows:

- $x_{p,t} \in \{0, 1\}$: This variable is equal to one if there is a electrolyser installed at location p and working at time t, otherwise it is zero.

- $hp_{p,t} \geq 0$: This variable determines the hydrogen production at electrolyser p and time t, in kg.

- $y_{p,f} \in \{0, 1\}$: This variable is equal to one if transportation between electrolyser p and hydrogen fuel station f has been established, and zero otherwise.

- $ht_{d,p,f} \geq 0$: This variable determines how much hydrogen was transported at a given day d from electrolyser p to fuel station f, in kg.

The objective function, equation 4.1, aims at minimizing the total cost of the entire supply chain.

$$\sum_{p \in P} PCC_p + CCC_s + SCC_s + TCC_s + \sum_{p \in P} POC_p + \sum_{p \in P} COC_{p,s} + SOC_s +$$

$$\sum_{p \in P} \sum_{f \in F} TOC_{p,f}$$

(4.1)

where,

PCC_p: Determines the production capital costs of electrolyser p, in €.

CCC_{LH_2}: Determines the conversion capital costs at liquid state, in €.

SCC_s: Determines the fuel stations' capital costs at state s, in €.

TCC_s: Determines the transportation capital costs at state s, in €.

POC_p: Determines the production operating costs of electrolyser p, in €.

COC_{p,LH_2}: Determines the conversion operating costs of electrolyser p at liquid state, in €.

SOC_s: Determines the fuel stations' operating costs at state s, in €.

$TOC_{p,f}$: Determines the transportation operating costs from electrolyser p to hydrogen fuel station f, in €.

The hydrogen supply chain comprehends production, conversion, transportation and refuelling stations costs. Each cost is broken down into capital and operational cost components as can be seen above. As mentioned, the centralised design was modelled for two possible states, s, namely gaseous and liquefied. In addition, it is important to underline that the hydrogen is assumed to be transported via delivery trucks.

All four components of capital costs include specific annual $O\&M$ costs, and annuity factors (AF). The annuity factors account for the depreciation of one-time investments over multiple years and depend on the weighted average cost of capital (WACC [%]) and the individual depreciation years $(d[-])$ [59], as shown in equation 4.2.

$$AF = \frac{(1 + WACC)^d * WACC}{(1 + WACC)^d - 1} \tag{4.2}$$

The electrolyser's capital costs can be calculated as shown in equation 4.3, which are adapted from [55].

$$PCC_p = \frac{IE * ED * Mhp_p}{EE} * (1 + O\&M_E) * AF_E \tag{4.3}$$

where,

IE stands for capacity dependent investment costs, in [€/kW].

Mhp_p stands for maximum hourly hydrogen production, in kg_{H_2}/h.

ED stands for hydrogen's energy density, in $[kWh_{H_2}/kg_{H_2}]$.

EE stands for the electrolyser efficiency, in $[kWh_{H_2}/kWh_{el}]$.

Conversion capital costs depend on capacity-specific investment costs, IC [€/kg_{H_2}], and the maximum daily sum of converted hydrogen across all plants, $MDhp$ [€/kg_{H_2}], equation 4.4. Conversion costs are only included when the supply chain design is modelled with hydrogen transportation in liquid state.

$$CCC_{LH_2} \; = \; IC_{LH_2}(MDhp) \; * \; (1 \; + \; O\&M_{C_{LH_2}}) \; * \; AF_C \qquad (4.4)$$

Fuel station capital costs equal the investment costs of one fueling station, IS €multiplied by the number of fueling stations NFS $[-]$, equation 4.5.

$$SCC_s = \; IS_s \; * \; NFS \; * \; (1 \; + \; O\&M_{S_s}) \; * \; AF_S \qquad (4.5)$$

Transportation capital costs equal the number of trucks and trailers, NT $[-]$, multiplied by the respective investment per truck $ITRU$ [€] and trailer $ITRA$ [€]. The number of trucks and trailers is equal to the number of hydrogen fuel stations, as it is assumed that a truck can supply only one fuel station, equation 4.6.

$$TCC_s = ITRU \; * \; NT \; * \; (1 \; + \; O\&M_{TRU}) \; * \; AF_{TRU} \; + \; ITRA_s \; * \; NT \; *$$

$$(1 \; + \; O\&M_{TRA_s}) \; * \; AF_{TRA} \qquad (4.6)$$

The production operating costs of each electrolyser depend on its hourly hydrogen output, $hp_{p,t}$ $[kg_{H_2}]$, the electricity consumption, ECP $[kWh_{el}/kg_{H_2}]$ and the location-specific electricity price, EP_p [€/kWh_{el}], equation 4.7.

$$POC_p = \sum_{t \in T} hp_{p,t} * ECP * EP_{p,t} \quad \forall\, p \in P \tag{4.7}$$

In addition, the model includes the operating costs of converting hydrogen. For liquid delivery, hydrogen needs to be liquefied and later evaporated at the location of consumption. Thus the costs depend on the daily hydrogen throughput, HP_p $[kg_{H_2}]$, the electricity required for liquefaction and evaporation ($EC_{liquefication}$ and $EC_{evaporation}$, both in $[kWh_{el}/kg_{H_2}]$) and the respective losses, equation 4.8.

$$COC_{p,LH_2} = (\sum_{t \in T} hp_{p,t} * EC_{liquefaction} * EP_{p,t} * (1 + Loss_{liquefaction}) +$$

$$\sum_{t \in T} hp_{p,t} * EC_{evaporation} * EP_{p,t} * (1 + Loss_{evaporation})) \quad \forall\, p \in P$$

$$\tag{4.8}$$

The fueling station operating costs are formed by the output-dependent consumption of electricity, $EC_{station_s}$ $[kWh_{el}/kg_{H_2}]$, and the respective price, EP $[€/kWh_{el}]$, equation 4.9.

$$SOC_s = (ECS_s * EP) * (1 + Loss_s) * \sum_{p \in P} \sum_{t \in T} hp_{p,t} \tag{4.9}$$

At last, the transportation operating costs are made up of labour costs (LC) as well as fuel and toll costs (FCT), equation 4.10. The fuel and toll costs are comprised of the transport distance between matched electrolysers and fueling stations ($TD_{p,i}$ $[km]$), fuel consumption (FC $[€/kg_{H_2}]$), fuel price (FP $[€/kg_{H_2}]$), and toll (TC $[€/km]$), equation 4.11. The labour costs are dependent on the driving time (DT $[h]$), which is made up of the transport distance ($TD_{p,i}$ $[km]$), average driving speed, (DS $[km/h]$), and hourly wage (W $[€/h]$), equation 4.12. The distances were computed using the Haversine Formula, which is accurate to around 0.3%, thus 1000 km has an error up to 3 km, which is assumed to be acceptable in this case. A more accurate formula to calculate the distance between two points on Earth's sphere is the Vincenty Formula, which is accurate to about 0.1mm, however, it takes more time and memory to run. The driving distance between two coordinates is seldom the closest distance between them. Thus, in line with [60], this heuristic has been taken into account by multiplying with a

CHAPTER 4. METHODOLOGY

detour factor of 1.3, equation 4.13. Both $FCT_{p,i}$ and $LC_{p,i}$ are multiplied by the ratio between the HRS capacity (HRS_{cap}) and the trailer's capacity according to the state s (T_{cap_s}).

$$TOC_{p,i} = (LC_{p,i} + FCT_{p,i}) * 365 \tag{4.10}$$

$$FCT_{p,i} = 2 * TD_{p,i} * 1.3 * Y_{p,i} * (FC * FP + TC) * \frac{HRS_{cap}}{T_{cap_s}} \tag{4.11}$$

$$LC_{p,i} = (2 * DT_{p,i} * W) * \frac{HRS_{cap}}{T_{cap_s}} \tag{4.12}$$

$$DT_{p,i} = TD_{p,i} * 1.3 / DS \tag{4.13}$$

4.1.1 Constraints

The daily transportation volume $ht_{d,p,f}$ between an electrolyser p and a hydrogen fueling station f is set to meet the daily demand of a fueling station $SCAP_d$ if connection is established between them. The daily demand $SCAP_d$ is the same across all fuel stations, however, it can be different depending on the day so as to account for seasonal variations, equation 4.14.

$$ht_{d,p,f} = SCAP_d * y_{p,f} \quad \forall \, d \in D, \, p \in P, \, f \in F \tag{4.14}$$

The sum of all transportation volume at a given day d must satisfy the hydrogen demand across all the hydrogen refuelling stations, equation 4.15.

$$\sum_{d \in D} ht_{d,p,f} \geq SCAP_d * NFS \quad \forall \, p \in P, \, f \in F \tag{4.15}$$

In sum, the daily amount of hydrogen transported from an electrolyser p to all fueling stations it supplies must not exceed its production, equation 4.18.

$$t_1 = d * 24 \quad \forall \, d \in D \tag{4.16}$$

$$t_2 = (d + 1) * 24 \quad \forall \, d \in D \tag{4.17}$$

$$\sum_{t_1}^{t_2} hp_{p,t} \geq \sum_{f \in F} ht_{d,p,f} \quad \forall \, d \in D, \, p \in P \tag{4.18}$$

The hydrogen output $hp_{p,t}$ of each electrolyser depends on its installed capacity, which lies between a fixed minimum and maximum value $HPCAP$. Besides, hydrogen output can only be non-zero if an electrolyser is installed at the respective location and working at time t, equation 4.19.

$$HPCAP_{\min} * x_{p,t} \leq hp_{p,t} \leq HPCAP_{\max} * x_{p,t} \quad \forall \, p \in P \tag{4.19}$$

The entire demand of a fueling station is covered by one electrolysis plant, equation 4.20.

$$\sum_{p \in P} y_{p,f} = 1 \quad \forall \, f \in F \tag{4.20}$$

The connection between an electrolyser p and fuel station f can only exist if the driving time is lower than 12 hours. This constraint ensures there is sufficient time for the truck to refuel the hydrogen fuel station at least once every day, equation 4.21.

$$DT_{p,f} > 12 \Rightarrow y_{p,f} = 0 \quad \forall \, p \in P, \, f \in F \tag{4.21}$$

4.2 Decentralised hydrogen design - optimisation formulation

The sets and indices of the optimisation are as follows:

- $f \in F = \{1, 2, ...99\}$: Index and set of hydrogen fuel stations.

- $t \in T = \{1, 2, ..., 8760\}$: Index and set of hours in a year.

- $d \in D = \{1, 2, ..., 365\}$: Index and set of days in a year.

The decision variables of the optimisation are as follows:

- $x_{f,t} \in \{0, 1\}$: This variable is equal to one if there is an electrolyser installed at location p and working at time t, and zero otherwise.

- $hp_{f,t} \geq 0$: This variable determines the hydrogen production at electrolyser p and time t, in kg.

The objective function, equation 4.22, is to minimize the total cost of the entire supply chain. There is no transportation as the hydrogen is produced on-site, and there are no conversion costs as there is no need to change its state into liquid. The necessary compression costs from the 30 bar outlet pressure of the electrolyser [61] to the 350/700 bar pressure required to fuel the trucks/cars are included in the fuel station investment cost [30].

$$\sum_{f \in f} PCC_f + SCC_s + \sum_{f \in f} POC_f + SOC_s \tag{4.22}$$

where,

PCC_f: Determines the production capital costs of hydrogen fuel station f, in €.

SCC_{GH_2}: Determines the fuel stations' capital costs at gaseous state, in €.

POC_f: Determines the production operating costs of hydrogen fuel station f, in€.

SOC_{GH_2}: Determines the fuel stations' operating costs at state gaseous state, in €.

As in the centralized model, all components of capital costs include specific annual O&M costs and annuity factors (AF) as in equation 4.2. The equations for the cost components 4.3, 4.5, 4.7 and 4.9 remain the same as in the centralized model, apart from the index, which changes to f, since there is on-site production. Therefore, the

on-site production capital costs and on-site production operational costs, PCC_f and POC_f can be calculated as in equations 4.23 and 4.24.

$$PCC_f = \frac{IE * ED * Mhfs_f}{EE} * (1 + O\&M_E * AF_E) \tag{4.23}$$

$$POC_f = \sum_{t \in T} hfs_{f,t} * ECP * EP_{f,t} \quad \forall \, f \in F \tag{4.24}$$

4.2.1 Constraints

The daily demand of every hydrogen fueling station, $SCAP_d$, must be satisfied by the on-site electrolyser at that same fuel station f.

$$t_1 = d * 24 \quad \forall \, d \in D \tag{4.25}$$

$$t_2 = (d+1) * 24 \quad \forall \, d \in D \tag{4.26}$$

$$\sum_{t_1}^{t_2} hp_{f,t} \geq SCAP_d \quad \forall \, f \in F, \, d \in D \tag{4.27}$$

The hydrogen output $hp_{f,t}$ of the electrolyser at each hydrogen fueling station f depends on its installed capacity, as in equation 4.19.

4.3 Mixed hydrogen design - optimisation formulation

The sets and indices of the optimisation are as follows:

- $p \in P = \{1, 2, ..., 222\}$: Index and set of potential electrolysis power plants.

- $f \in F = \{1, 2, ...99\}$: Index and set of hydrogen fuel stations.

- $t \in T = \{1, 2, ..., 8760\}$: Index and set of hours in a year.

- $d \in D = \{1, 2, ..., 365\}$: Index and set of days in a year.

The decision variables of the optimisation are as follows:

- $x_{p,t} \in \{0, 1\}$: This variable is equal to one if there is a electrolyser installed at location p and working at time t, and 0 otherwise.

- $hp_{p,t} \geq 0$: This variable determines the hydrogen production at electrolyser p and time t, in kg.

- $y_{p,f} \in \{0, 1\}$: This variable is equal to 1 if transportation between electrolyser p and hydrogen fuel station f has been established, and 0 otherwise.

- $ht_{d,p,f} \geq 0$: This variable determines how much hydrogen was transported at a given day d from electrolyser p to fuel station f, in kg.

- $x_{f,t} \in \{0, 1\}$: This variable is equal to one if there is on-site production at fuel station f and working at time t, and 0 otherwise.

- $hfs_{f,t} \geq 0$: This variable determines the hydrogen production at fuel station f and time t, in kg.

- $select_f \in \{0, 1\}$: This variable is equal to one if that hydrogen fuel station f is to be supplied by on-site production, and zero otherwise.

The Objective function is to minimize the total cost of the entire supply chain.

$$\sum_{p \in P} PCC_p + \sum_{f \in F} PCC_f + SCC_{GH_2} + TCC_{GH_2} + \sum_{p \in P} POC_p +$$

$$\sum_{f \in F} POC_f + SOC_{GH_2} + \sum_{p \in P} \sum_{f \in F} TOC_{p,f} \tag{4.28}$$

where,

PCC_p: Determines the production capital costs of electrolyser p, in €.

PCC_f: Determines the production capital costs of the on-site electrolyser at hydrogen fuel station f, in €.

SCC_{GH_2}: Determines the fuel stations' capital costs at gaseous state, in €.

TCC_{GH_2}: Determines the transportation capital costs at gaseous state, in €.

POC_p: Determines the production operating costs of electrolyser p, in €.

POC_f: Determines the production operating costs of the on-site electrolyser at hydrogen fuel station f, in €.

SOC_{GH_2}: Determines the fuel stations' operating costs at gaseous state, in €.

$TOC_{p,f}$: Determines the transportation operating costs from electrolyser p to hydrogen fuel station f, in €.

The cost components are a merge of the centralised and decentralised design costs. Actually, in the objective function we can see the costs that came from the centralised design (equations 4.3, 4.5, 4.6, 4.7 and 4.9), plus the production costs that come from the decentralised design (equations 4.23 and 4.24).

There is a slight change within the transportation capital cost, in comparison to the centralised design, concerning the number of trucks and trailers. In the centralised design, the number of trucks and trailers is assumed to be the same as fuel stations. However, in the mixed design that is not the case as there may be on-site production. Hence, the number of trucks and trailers is given by equation 4.29.

$$NT = \sum_{p \in P} \sum_{f \in F} y_{p,f} \tag{4.29}$$

4.3.1 Constraints

As in the centralized model, the daily transportation volume HT between an electrolyser p and a hydrogen fueling station f is set to meet the daily demand of a fueling station $SCAP_d$ if connection is established between them (equation 4.14). The daily demand $SCAP_d$ is the same across all fuel stations, however, it can be different depending on the day so as to account for seasonal variations, equation 4.30.

$$ht_{d,p,f} \; = \; SCAP_d \; * \; y_{p,f} \quad \forall \, d \in D, \; p \in P, \; f \in F \tag{4.30}$$

As in the centralized model, in sum, the daily amount of hydrogen transported from an electrolyser p to all fueling stations it supplies must not exceed the production at this electrolyser (equation 4.15).

The on-site hydrogen production must satisfy the daily demand of hydrogen fuel station f if on-site production is chosen, equations 4.31 and 4.32.

$$aux_{d,f} = SCAP_d \; * \; select_f \quad \forall \, f \in F, \; d \in D \tag{4.31}$$

$$\sum_{t_1}^{t_2} hfs_{f,t} \geq aux_{d,f} \quad \forall \, f \in F, \; d \in D \tag{4.32}$$

The sum of all centralized and decentralized production must satisfy the daily hydrogen demand, 4.33.

$$\sum_{p \in P} \sum_{f \in F} ht_{d,p,t} + \sum_{f \in F} aux_{d,f} \geq SCAP_d * NFS \quad \forall \, d \in D \tag{4.33}$$

Both the hydrogen output $hp_{p,t}$ and $hfs_{f,t}$ depend on their installed capacities, as in equation 4.19.

As in the centralized model, connection between an electrolyser p and fuel station f can only exist if the driving time is lower than 12 hours (equation 4.21).

The entire demand of a fuel station can be covered by at most one electrolysis power plant p, equation 4.34.

$$\sum_{p \in P} y_{p,f} \leq 1 \quad \forall \, f \in F \tag{4.34}$$

24

4.4 Hydrogen supply chain data

In this section, the relevant data as well as the steps and assumptions needed to build the hydrogen model are described.

4.4.1 Hydrogen Demand Data

Firstly, the hydrogen demand in 2030 for trucks and passenger vehicles was acquired through a study commissioned by The Fuel Cells and Hydrogen Joint Undertaking (FCH JU) alongside the European Commission - DG Energy [62]. The aim of this study was to analyse the opportunities for hydrogen deployment on a nationwide scale as well its impacts on the nation's economic, environmental and technical spheres through the development of a high and low hydrogen penetration scenario. In this study, it was assumed the high penetration scenario.

The relevant data of this study is the number of forecasted fuel cell electric trucks and passenger vehicles. With such data it is possible to estimate the annual hydrogen demand for this sector by using the average consumption [63], [64] and average mileage during the period of one year [65]. The estimations can be seen in the tables below.

	Heavy duty trucks	Passenger vehicles
Average mileage [km]	40410	11000
Average consumption [kg/100km]	8	0.63

Table 4.1: Average consumption and average mileage of heavy-duty trucks and passenger vehicles.

Heavy duty trucks		Passenger vehicles	
Number of vehicles	H2 annual demand [ton]	Number of vehicles	H2 annual demand [ton]
7200	23276	103700	7186

Table 4.2: Hydrogen annual demand (in tons) for heavy-duty trucks and passenger vehicles.

As mentioned, every hydrogen supply chain design was parameterized for two differ-

ent scenarios, one considering seasonal variation and the other that does not. Regardless of the variations, the annual hydrogen demand is the same for both scenarios and is equal to a combined value (from both trucks and passenger vehicles) of 30 462 tons.

Scenario without seasonal variation - Under this scenario, the daily hydrogen demand is computed by simply dividing the annual hydrogen demand by the number of days in a year (365). Hence, the average daily consumption of heavy-duty trucks and passenger vehicles is 63.7 tons and 19.7 tons, respectively.

Scenario with seasonal variation - The hydrogen annual demand must be transformed into a daily demand and if possible, depict its fluctuations over the entire year as closely as possible to reality. The hydrogen demand is dependent on two parameters, consumption and mileage. According to the study performed by Vepsäläinen et al. on battery electric buses, the consumption is dependent on several factors, the most important being the outside ambient temperature. Actually, its variation contributed to almost 60% of the entire energy consumption [66]. In this study, Vepsäläinen et al. provided a graph depicting the fluctuation in energy consumption based on ambient temperature. The energy consumption displayed a range of values for each ambient temperature value. Based on that graphic Jacob [67] arrived at an equation to calculate the hydrogen demand of a fuel cell electric bus (FCEB), eq 4.35. The outside temperature was used to compute seasonality in hydrogen demand was as it seemed a reasonable proxy to use the work of [66], even though it is related to buses. No other factors, such as traffic seasonality was taken into account since it could not be found reliable and accurate data.

$$FCEB_{consumption} = (3.84 * 10^{-6}T^3 + 2.14 * 10^{-4}T^2 - 6.84 * 10^{-2}T + 1.0397) \quad (4.35)$$

Where $FCEB_{consumption}$ stands for the energy demand of the battery electric bus, in $[kg_{H_2}/km]$, and T denotes the ambient temperature in [ºC].

The data regarding ambient temperature according to the season was acquired from the SMHI (the Swedish Meteorological and Hydrological Institute). In short, a daily average ambient temperature for the Örebro municipality in 2021 was computed using the hourly ambient temperature recorded that year [68]. The Örebro municipality was used as a reference to get the ambient temperature variance as it is located in the centre of the South of Sweden where most traffic is assumed as it will be described in the following paragraphs. Consequently, the daily average consumption per 100km was computed by means of the equation above and the average consumption across all the days in the year was $6.71 \ kg_{H_2}/100km$. It's important to highlight that this equation is meant to be used for the consumption of buses, hence, to depict the consumption variation for trucks, all the values for the daily average consumption were multiplied by

$8/6.71$ in order to get an average consumption across all the days of $8\ kg_{H_2}/100km$. The same procedure was used for passenger vehicles, however, in this case, the intended average consumption across all the days was $0.63\ kg_{H_2}/100km$.
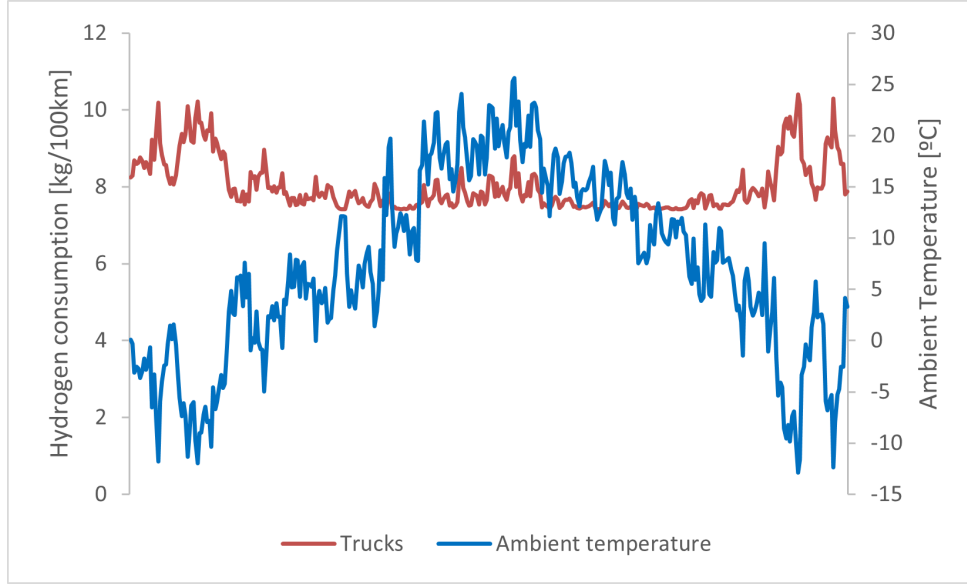
(a)
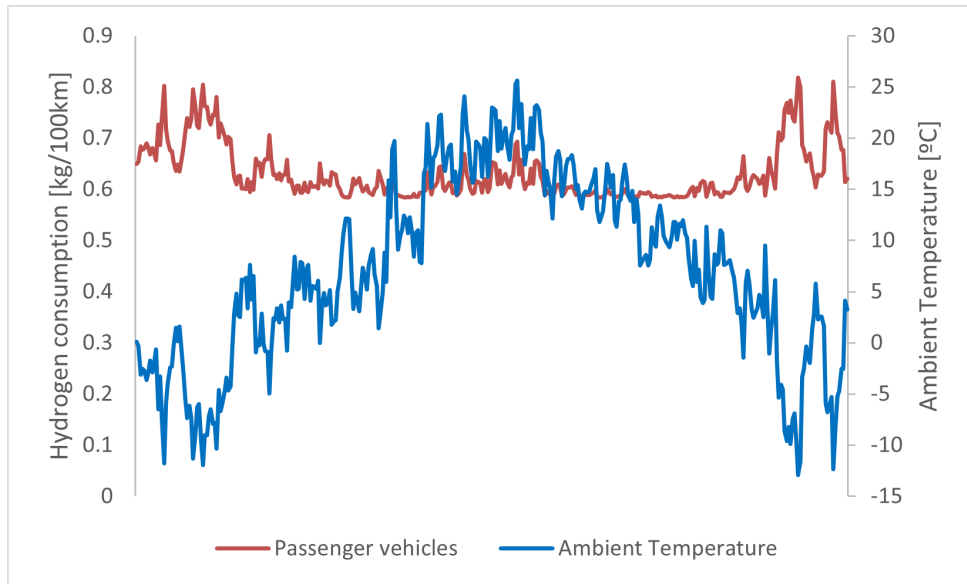
(b)

Figure 4.3: Average consumption seasonality, for trucks (a) and passenger vehicles(b), according to ambient temperature.

The estimated hydrogen daily demand must be spatially divided, which was done

according to the population density of Sweden. Sweden is regionally divided according to the NUTS (Nomenclature of Territorial Units for Statistics) methodology. In order to have a reasonably detailed distribution of the hydrogen demand, such distribution was done using the NUTS-3 level, in other words, the hydrogen demand was divided by county according to the population density of each county.

Once in possession of the daily hydrogen demand for each county, it becomes possible to estimate the number of HRSs to be deployed. It was assumed that by 2030 all HRS would become L-size, according to [30], which means maximum throughput capacities of 1000 kg/day. The required number of fuel stations is, therefore, equal to the maximum hydrogen daily demand divided by the fuel stations' maximum capacity of 1000 kg. This results in 90 hydrogen fuel stations regarding the scenario without seasonal variation and 109 hydrogen fuel stations regarding the scenario with seasonal variation.

In order to compute the capital costs of the hydrogen fuel stations, according to [30], equation 4.36 is used to estimate the investment cost per fuel station considering scaling and learning effects. At $n = 90$ and $n = 109$ stations, for scenario without seasonal variation and scenario with seasonal variation respectively, capacity $C = 1000$ kg/ day and the exogenous parameters α, β, and γ presented in Table 4.3 , it is possible to derive the investment cost per station for each hydrogen transportation state $s(s \in \{GH2, LH2\})$, as can be seen in Table 4.4.

$$IS_s = 1.3 * 600,000 EUR * \gamma * \left(\frac{C}{212kg/day} \right)^\alpha * (1 - \beta)^{\log_2 \left(\frac{C*n}{212kg/day*400} \right)} \quad (4.36)$$

Parameters	GH2	LH2
$\alpha[-]$	0.7	0.6
$\beta[-]$	0.06	0.06
$\gamma[-]$	0.6	0.9
ECS $[kWh_{el}/kg_{H_2}]$	1.6	0.6
GCS cons. $[kWh_{NG}/kg_{H_2}]$	0	0
Depreciation years $[a]$	10	10
O&M [%]	5	5

Table 4.3: Hydrogen fuel stations parameters according to the hydrogen state [30].

State	IC [M€] - scenario A	IC [M€] - scenario B
$H_2(g)$	1.38	1.36
$H_2(l)$	1.77	1.74

Table 4.4: Investment cost per hydrogen fuel station according to its state.

For heavy-duty trucks, the location of the HRS will be, preferentially, as close as possible to highways, plus, the possible locations of the HRS are assumed to be the locations of existing petrol fuel stations. Hence, OpenStreetMap was used to acquire both the location of existing petrol fuel stations and highways in each county. At first, the criteria to choose which petrol fuel stations would also become an HRS was proximity, in other words, fuel stations were chosen from closest to farthest until the required number of fuel stations was met. Then a second criterion was implemented, it ensured each HRS could not be within a radius of x km to another HRS.

The span of the radius depends on the county as there are counties with a large area and few HRS stations which is the case of Norbotten county while other counties such as Stockholm are quite smaller in area however a lot more HRS were allocated there. Therefore, the chosen radius in counties like Norbotten is larger than in counties like Stockholm. Setting the radius was achieved through the following method: after setting a certain radius, a map of the HRS in the respective county was plotted and visually analysed. If any of the chosen HRS was far from any of the highways, the radius was decreased until all HRS were lying next to highways and sufficiently apart from each other. On the other hand, if two or more of the HRS were close to each other, the radius was increased until they were sufficiently far apart and still in close proximity to highways. Thus, the process was only concluded once a radius was set that ensures a reasonably spatial HRS' distribution while also ensuring that the HRS were still quite close to the existing highways.

Regarding hydrogen fuel stations for passenger vehicles, these were distributed in each county according to the following example. Four HRS were set to be deployed in Stockholm County, and are spatially distributed by allocating a single HRS to each municipality starting with the municipality with the highest population. In this case, as there are only four HRS to be deployed, one HRS is allocated to the four municipalities with the highest population in Stockholm's County.

4.4.2 Hydrogen Production Data

Electrolysis utilizes electricity ("power") to split water into hydrogen and oxygen ("gas"). This power-to-gas process is at the center of long-term strategies for low-carbon hydrogen supply in the European Union [69], and consequently, the study considered hydrogen

production via electrolysis. Among the existing electrolysis technologies, proton exchange membrane (PEM) electrolysis shows a high technology readiness level, high potential for cost reduction and efficiency improvement [70] as well as high operational flexibility [21]. Besides, green hydrogen project developers are mostly choosing proton exchange membrane electrolysis over other technologies, such as alkaline technology [71], hence, the study focused on PEM electrolysis.

It was assumed investment costs IE of 500 €/kW_{el}, depreciation over 10 years, O&M costs of 3% of investment costs and an electricity consumption of $47.6\ kWh_{el}/kg_{H_2}$, based on [72]. For the centralized model, the minimum capacity of an electrolyser $HPCAP_{\min}$ was set to 10MW and the maximum $HPCAP_{\max}$ to 100MW, whereas for the decentralized model the minimum capacity was set to 2MW and maximum capacity to 4MW. The energy density of hydrogen is 33.33 kWh_{H_2}/kg_{H_2}.

For the centralized and mixed models, the potential locations for deploying the centralised electrolysis plants were considered to be the locations of transmission grid substations.

4.4.3 Hydrogen Transportation data

The transportation module of the hydrogen supply chain has been developed considering distribution via delivery trucks. Sweden doesn't exhibit a pipeline infrastructure such as the scope of other studies, like Germany for instance. Consequently, this model does not include pipeline distribution, only distribution via delivery trucks.

Due to hydrogen's low density, it is commonly transported in gaseous state or liquefied instead. Conversion assumptions are adopted from [60] and are presented in table 4.5. The variable x denotes the desired output of hydrogen. Regarding the scenario without seasonal variation, as the daily hydrogen demand is the same across all days, the x is equal to that daily hydrogen demand. Nevertheless, the scenario with seasonal variation intends to depict days with higher hydrogen demand than others, thus the conversion facilities must be able to convert the amount of hydrogen corresponding to the day where the demand is maximum. Hence, x is equal to the maximum daily hydrogen demand.

In the next step, hydrogen is filled into trailers and transported to fueling stations via delivery trucks. Fuel consumption of a delivery truck is set to 8 $kg_{H_2}/100$ km. Besides fuel costs, toll costs (0.15 €/km) were also included as well as labor costs of 20 €/$hour$ for the transportation, based on [55], [73]. The investment cost per truck was assumed to be 160.000 €, depreciation over eight years, and 12% O&M costs. Moreover, trailer

costs were assumed to be 660.000 € for $H_2(g)$ and 860.000 € for $H_2(l)$ [30].

The trailer's maximum capacity is, according to the two different states, 1100 kg_{H_2}, 4300 kg_{H_2}, respectively [30]. For the purpose of this study, the trailer capacity for gaseous state was assumed to carry a maximum of 1000 kg_{H_2}, and for liquid state 4000 kg_{H_2}. Furthermore, each truck only provides hydrogen to one fuel station, and the driving distance between electrolyser p and HRS f must be within 12 hours. Although the model simulates that a truck does not have to travel back every day in order to refill the HRS, this constraint is important in order to ensure that there is sufficient time for the truck to travel to the HRS facility and back within one day. For instance, regarding the centralised design in scenario without seasonal variation, if hydrogen is transported in gaseous state, the trailers have 1000 kg capacity and since the HRS have a 1000 kg/day capacity, then the trucks must be able to travel from the electrolyser facility to the HRS and back within one day to ensure the HRS is supplied every day. If hydrogen is transported in liquid state, the trailers have a 4000 kg capacity and thus are able to remain at the HRS. However, every four days, the truck must travel back to electrolyser facility, and back again to the HRS in order to ensure that the HRS is supplied with hydrogen for the next day. Consequently, the model ensures that every day each HRS is supplied with the respective demand, and besides, the number of trucks and trailers required is the same number as HRS.

	Investment Cost [M€]	Depreciation years	O&M	Elect. consum. [kWh/kg]
Liquification	$1.05 * 10^8 * \left(\dfrac{x}{50 \frac{t_{H_2}}{day}} \right)^{0.66}$	20	4%	6.78
Evaporation	$3 * 10^3 * \left(\dfrac{x}{\frac{t_{H_2}}{day}} \right)$	10	3%	0.6

Table 4.5: Conversion assumptions, adopted from [30].

4.5 Electricity system model

The electricity market in Sweden has four zones, called bidding zones, which can have different prices, namely SE1, SE2, SE3 and SE4. The electricity system was modelled to simulate hourly electricity prices, according to each zone, which will be used as inputs for the Hydrogen models. In addition, the model will be used later to measure the impact of the hydrogen demand on electricity prices.

Nord Pool provides a map depicting the four different bidding zones in Sweden as

can be seen in figure 4.4a. The bidding zones' borders or areas are important in order to assign each transmission grid node to the bidding zone it belongs to. There is no data source that provides the bidding zones' borders/areas in any way besides in a map format as in the Nord Pool map. Thus, Global Mapper was used to acquire the bidding zones' areas, as it can be seen in figure 4.4b, based in the Nord Pool map.

(a)   (b)
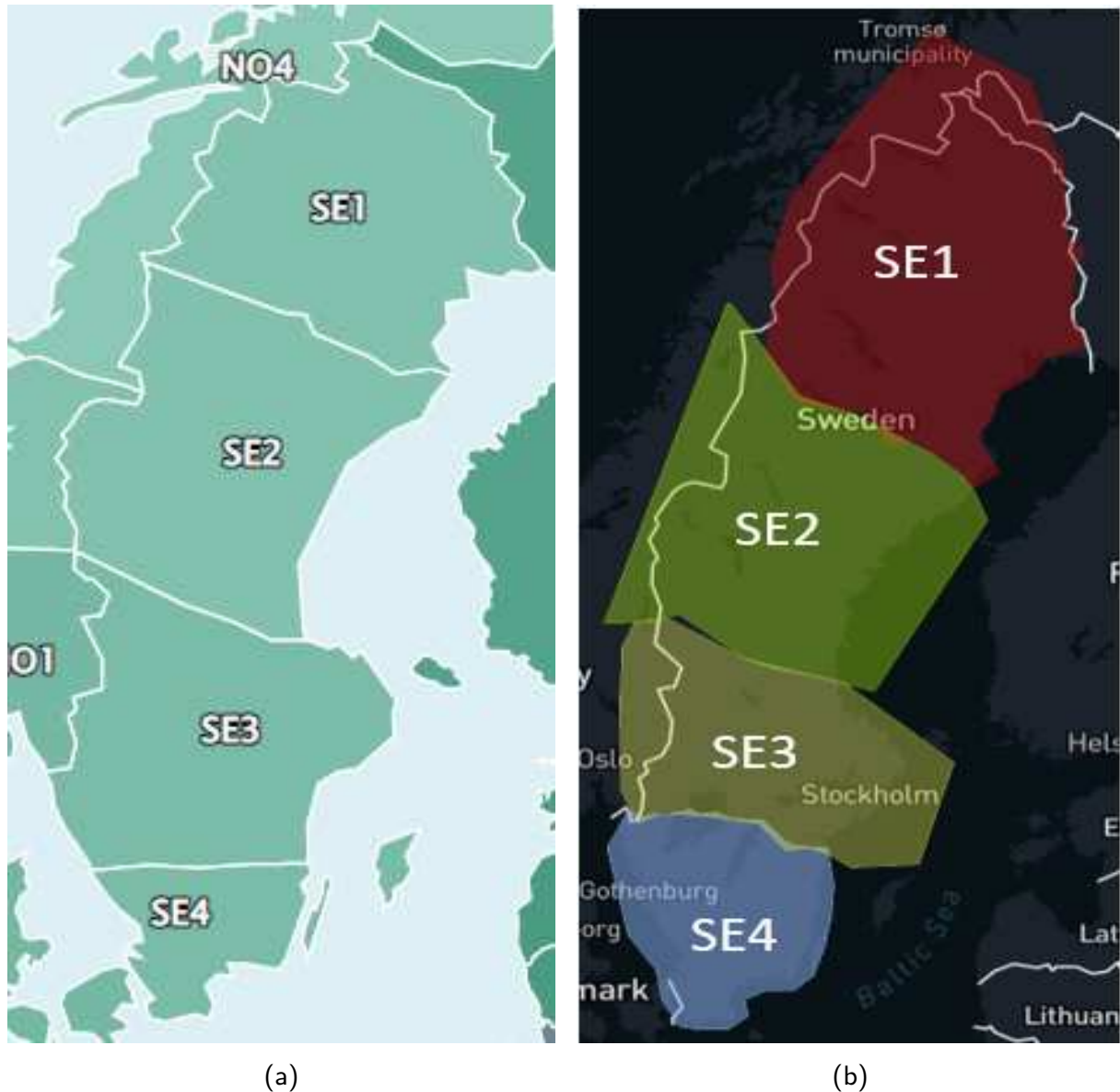
Figure 4.4: Bidding zones in Sweden according to Nord Pool (a) and respective areas acquired with Global Mapper (b).

4.5.1 Transmission grid

The transmission grid is managed by Svenska kraftnät, which is a state-owned enterprise, and among other things, it's tasked with maintaining Sweden's electricity transmission grid. Other responsibilities of Svenska kraftnät include the development of the transmission grid in order to meet society's demands for a secure, sustainable and cost-effective supply of electricity. Thus, Svenska kraftnät is positioned in a way that plays an important role in implementing national climate policies. Besides it is the country's only TSO [74].

The transmission grid was modelled via the PyPSA-eur model, which creates the transmission grid model by extracting it from the ENTSO-E interactive map of the European power system [75]. There are some limitations to modelling the transmission grid from this ENTSO-E extract, such as:

- Geographical coordinates are transferred from the ENTSO-E map, which is known to choose topological clarity over geographical accuracy. Hence coordinates will not correspond exactly to reality.
- Voltage levels are typically provided as ranges by ENTSO-E, of which the lower bound has been reported in this dataset.
- Line structure conflicts are resolved by picking the first structure in the set.
- Transformers are not present in the original ENTSO-E dataset, their presence has been derived from the different voltages from the connected lines.
- The connection between generators and busses is derived as the geographically nearest station at the lowest voltage level. This information is again not present in the ENTSO-E dataset.

Since this study is being conducted for a 2030 scenario, future grid expansions should be included in the model, which will be done according to [74]. Following [76], [77], we approximate the transmission capacity of all 220 kV lines to be 490 MW, and that of all 380-400 kV lines to be 1700 MW. Multiple lines between two nodes are aggregated into one by summing up the capacity value.

The transmission grid including the planned expansions for 2030 is depicted below. In green, we can see the 220 kV lines and in red the 400 kV ones, the white dots represent the grid's nodes. There is not a major expansion of the grid, and it was mainly focused near Stockholm as planned in [74]. The TSO proposes, however, to renew many of the transmission cables, which are quite old, thus increasing the transmission capacity of the grid.
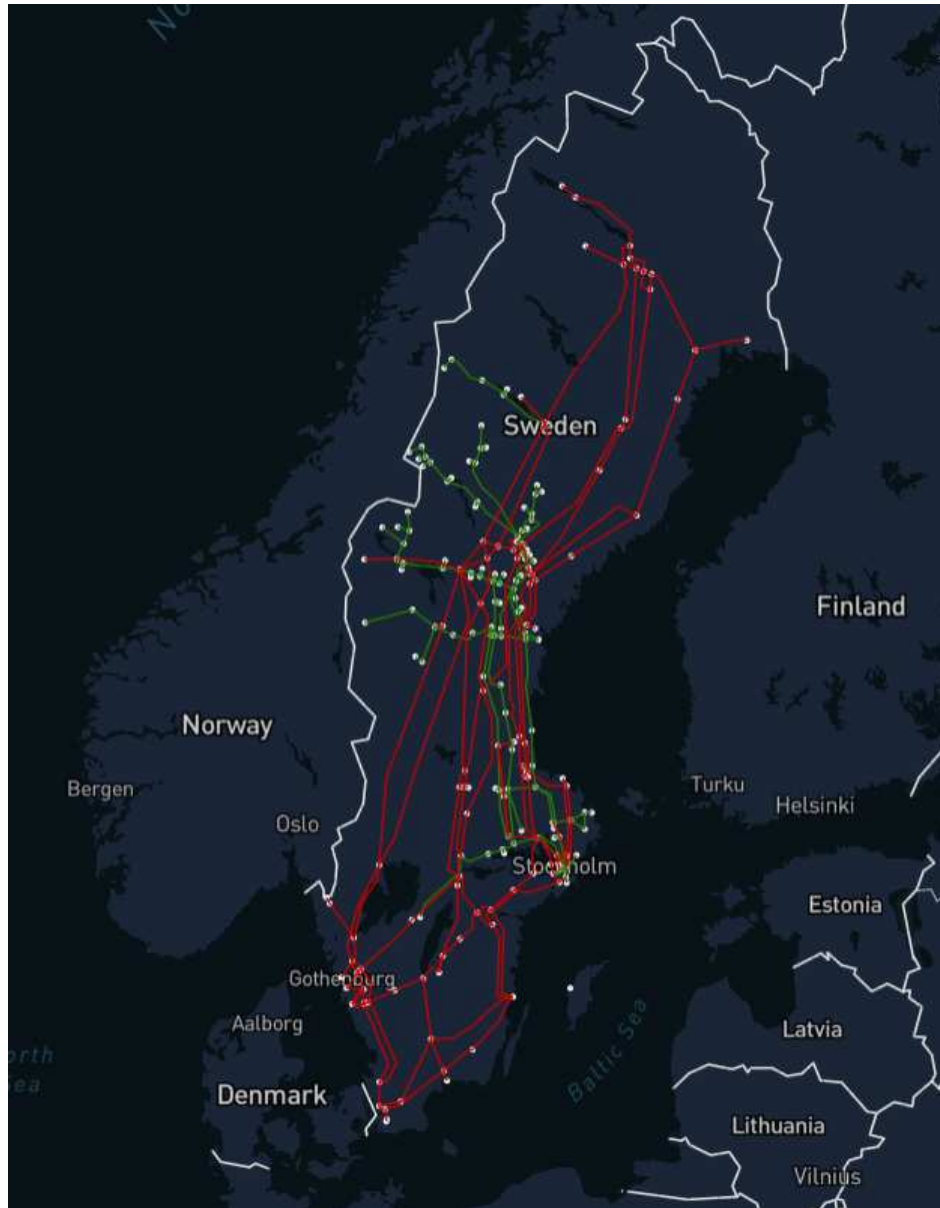
Figure 4.5: Transmission grid in Sweden, including expansions by 2030.

4.5.2   Hourly load demand in each bidding zone

The hourly load demand in each zone in 2030 was estimated through data made available by ENTSO-E [78]. ENTSO-E offers hourly load demand forecasts for 2030 considering three different scenarios, in this case, the "EUCO30" scenario was chosen which assumes that the 2030 climate and energy targets as agreed by the European Council in 2014 were achieved. For Sweden, the scenario includes three different variations of hourly demand

forecasts in each zone, each variation representing the climatic conditions of different years, 1982, 1984 and 2007. The three variations are averaged as in equation 4.37, in order to depict the load demand of an average climatic year, according to [79].

$$Load_{h,zone,2030} = \frac{1}{3} * (Load_{h,zone,2030,1982} + Load_{h,zone,2030,1984} + Load_{h,zone,2030,2007})$$

$$(4.37)$$

The resulting total electricity demand in Sweden in 2030 is, based on the estimation above, 159 TWh. The hourly load demand series acquired were already separated by bidding zone.

4.5.3 Temporal distribution of electricity generation from RES

In this section, a detailed description will be provided of how the installed capacity of wind, solar and hydroelectric energy in Sweden in 2030 was retrieved as well as the respective hourly generation profiles.

Global Data produced a report stating that Sweden's renewable energy capacity, excluding hydropower, will reach 30.4 GW by 2030. More precisely, it shows solar and wind power to grow by an annual compound growth rate (CAGR) of 16% and 8.3% over the 11-year period [80].

In order to have full access to the report it has to be purchased, however, with the information contained in the above paragraph, it is possible to compute the required data, such as the solar and onshore wind installed capacity by 2030. Following the annual compound growth rate formula and knowing the starting value it is possible to arrive at the forecasted capacity for both solar and onshore wind technologies [81]. According to the Swedish Wind Energy Association, the starting value for the wind power capacity forecast is 9.06 GW for the year 2019 [82], which means that in equation 4.38, t is equal to 11, resulting in a total installed capacity of 21.8 GW by 2030. Regarding solar energy, the starting value is 0.698 GW [83], [84], again $t = 11$, yielding a total installed capacity of 3.6 GW by 2030.

$$CAGR = \left(\frac{V_{\text{final}}}{V_{\text{start}}}\right)^{1/t} - 1 \qquad (4.38)$$

$V_{start} =$ starting value, $V_{final} =$ final value, $t =$ time in years.

The next step consisted of building the generation profile for both solar and wind power plants. In this step, it was assumed that the temporal distribution of these variable sources will not change significantly over the next years. Consequently, historical time series from 2019, 2020 and 2021, which are available in [85], were used to build the wind energy generation profiles for 2030. First, the hourly generation values of the three years were averaged as in the equation below, although, 2020 was a leap year and consequently the hourly values corresponding to the 29th of February were removed from the data before averaging.

$$Generation_{h,avg_{19,20,21}} = \frac{(Generation_{h,2019} + Generation_{h,2020} + Generation_{h,2021})}{3}$$

$$(4.39)$$

Then, since the total electricity generation in 2030 will be different than in the other years, the hourly generation values must be refactored. In order to perform the re-factorization, the average of the total generation for the three years was calculated as well as the total estimated generation for 2030 [79]. Technical progress is expected to increase the capacity factor of wind turbines to 40% in 2025 and 45% in 2030 [86]. Nevertheless, since wind turbines deployed in previous years such as 2015 present a capacity factor of 26%, it was assumed an average capacity factor of 35%. Thus, assuming a net capacity of 21.8 GW and a capacity factor of 35%, the projected wind energy generation for 2030 resulted in 66.8 TWh. At last, the hourly generation for 2030 was refactored following the equation below.

$$Generation_{h,2030} = Generation_{h,avg_{19,20,21}} * \frac{TotalGeneration_{2030}}{TotalGeneration_{avg_{19,20,21}}} \quad (4.40)$$

The hourly generation data imported from the ENTSO-E database did not, unfortunately, present any data regarding solar production, hence, the generation profile of solar energy was acquired with PVGIS [87].

It was assumed that the solar energy generation for 2030 would also be built based on three reference years, and since the SARAH2 database only had data until 2020, the chosen years were 2018, 2019 and 2020. For each year, the database only contained the solar radiation of that year and the peak power was set to be the installed capacity at that year, which was taken from [84]. Furthermore, it is important to highlight that the chosen location of the PV facility was in the middle of Jönköping County, as it is reasonably centred in the south of Sweden, accordingly to the assumption mentioned in section 4.5.4. The annual electricity generation values prompted by the PVGIS tool do not differ significantly from the actual electricity generated from solar energy.

The same steps were followed for the estimated wind energy generation in 2030, however this time the capacity factor was assumed to be 11% as it seems to be a reasonable value since the capacity factors for the years 2018, 2019 and 2020 were 11%, 8% and 11% respectively. The estimated electricity generation from solar energy in 2030 was then 3.5 TWh.

Regarding hydropower, the total installed capacity nowadays, roughly 16 GW [88], is expected to remain unchanged by 2030. Being an intermittent and variable energy source, in order to depict its availability, the hydropower hourly generation profile was computed by averaging the hourly values of the years 2017 to 2021 from the ENTSO-E database. There was no need to do any refactorization as the installed capacity was the same for the respective years. The resulting total hydropower generation forecasted for 2030 yields a possible maximum of 68 TWh.

4.5.4   Spatial distribution of electricity generation

The electricity generation must be spatially distributed and assigned to transmission grid nodes. Nuclear power plants and fossil-based power plants are already assigned to the respective transmission grid nodes through the PyPSA-Eur model. There are six nuclear power plants operating in Sweden as of June 2022, and it is assumed that they will remain as it is in 2030. Thus, meaning a total installed capacity of 6.8 GW, divided in 3.2 GW in zone SE3 and 3.6 GW in zone SE4. Fossil-based power plants are located in zones SE3 and SE4 with respective capacities of 1.7 GW and 1.5GW. The bio-energy power plants in Sweden included in the PyPSA-Eur model are very scarce and the total installed capacity is very far from reality. Nevertheless, Energiföretagen, has divulged in the report [89] the installed capacity of bio-energy power plants in each bidding zone of Sweden. This data does present one limitation: on occasions when there is a great need for district heating some of the capacity is diverted from electricity generation to heat generation. This fact was not taken into account and it is assumed that the entire capacity is available at any time for electricity generation. The bio-energy installed capacity is 272 MW, 682 MW, 2816 MW and 1549 MW for zones SE1, SE2, SE3 and SE4 respectively.

Despite knowing roughly how much wind capacity should be installed by now, there is also a lack of available information regarding wind turbines' locations, coordinate-wise, and corresponding capacities. The most detailed available source is OpenStreetMap, which is susceptible to incomplete and inaccurate information. Using the overpass-turbo tool, wind turbines were filtered from OpenStreetMap, resulting in a total of 3882 wind turbines. This number is not in accordance with the official source [90], which states that by July 2021 more than 4000 had been deployed in Sweden. Even though there is this discrepancy from OpenStreetMap, due to the lack of better sources, the wind turbines'

locations from OpenStreetMap will be used to spatially distribute wind capacity.

Some wind turbines, besides providing coordinates, also indicate the corresponding capacities. However, the vast majority don't, which makes it impossible to know how much wind capacity still needs to be distributed in order to reach the 2030 target. Therefore, it was assumed that the wind turbines had been deployed by the end of 2021 resulting in a total capacity of 10.6 GW according to the CAGR formula. Thus, the capacity for the wind turbines without known capacity was assumed to be 2.6 MW so the sum of all wind turbines yielded the respective 10.6 GW. Afterwards, each wind turbine was assigned to its closest node using the Haversine formula, that has been explained in section 4.1,which allowed to compute how much capacity was assigned at each node.

There is still 11.2 GW of wind capacity left to allocate in order to reach the 21.8 GW set for 2030. Sweden's transmission system operator, Svenska kraftnät, developed a report for the period of 2022 to 2031, which states that it is currently working to connect 8 GW of onshore wind capacity to the grid, particularly in zones SE1 and SE2 [91].
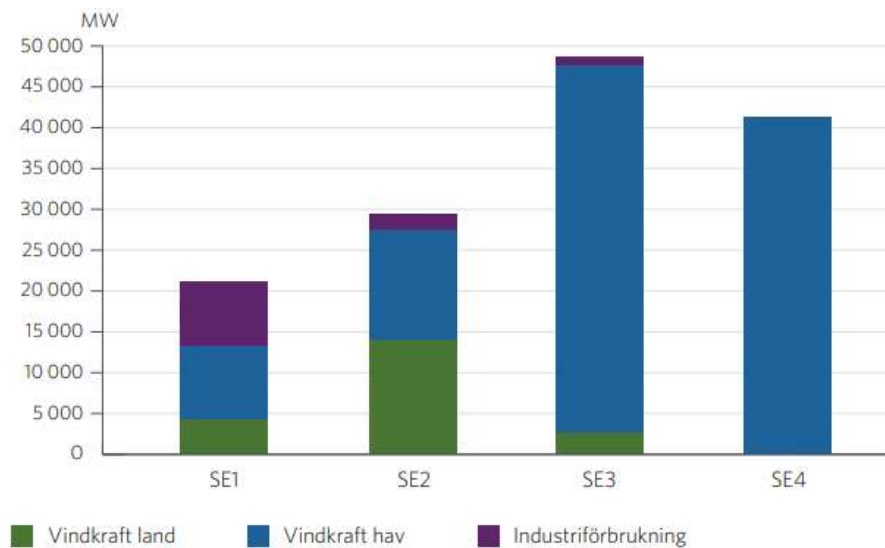
Figure 4.6: Total applied power in the investigation phase divided by electricity areas[91].

The figure 4.6 shows how much wind capacity has been applied to connect to the grid, onshore wind is depicted in green while offshore in blue. It clearly denotes that zone SE2 has the most applications for onshore wind, followed by zones SE1 and SE3. In order to allocate future wind capacity, in each zone, proportionally to the applications, the application's capacity in each zone was multiplied by 8 GW and then divided by the total of onshore wind applications across every zone. Thus, yielding 5.4 GW, 1.6 GW and 0.98 GW in zones SE2, SE1 and SE3 respectively. The wind capacity at each zone was distributed by scaling, evenly, the capacity of every node within each zone until meeting

that value.

At this stage, only 3.2 GW were left to be distributed. It was assumed that this capacity would regard only offshore wind and for zones SE3 and SE4 exclusively. It can be observed in figure 4.7 that offshore wind farms are expected to be deployed in the coming years. It was also assumed that the capacity was deployed evenly for both zones, in other words, 1.6 GW of offshore wind capacity for each zone. As shown in the figure, zone SE3 presents two different areas for the deployment of offshore wind, east and west, both were assigned with a 0.8 GW capacity. Zone SE4 presents three different areas, each assigned with 0.533 GW.
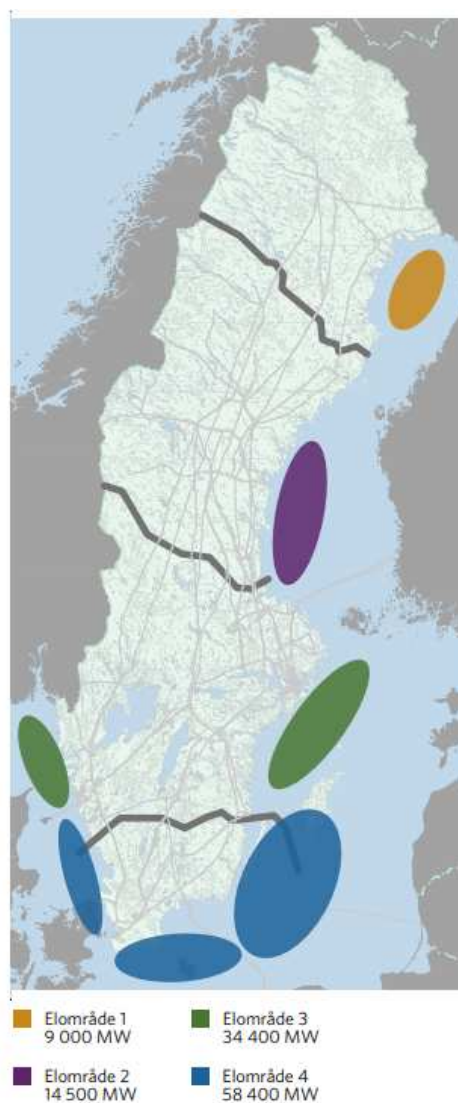
Figure 4.7: Applications for the connection of offshore wind power per electricity [91].

At last, the hourly wind energy generation at each node was assigned proportionally to the capacity at that same node. In other words, the installed wind capacity weight at each node was calculated (installed wind capacity at node divided by overall installed wind capacity) and multiplied by the hourly wind generation in 2030 described in the previous section.

$$WindGeneration_{h,node,2030} = \frac{WindCapacity_{node,2030}}{TotalWindCapacity_{2030}} * Generation_{h,2030} \quad (4.41)$$

Concerning solar energy, the Swedish Energy Agency provides information regarding how much solar energy is installed in each county and each municipality for the years 2016 and on-wards [92].

By having the installed capacity of each municipality, it is a reasonable assumption to assign the capacity in each municipality to its closest node. According to data retrieved above, the total installed capacity in Sweden in 2021 was 1.6 GW, therefore, 2 GW are still left to be assigned. Currently, in Sweden there is a spatial imbalance in the production and consumption of electricity, most of it is produced in the north region of Norrland, while most of its consumption is done in the South, where most of Sweden's population lives [93]. Since solar energy presents more potential to be deployed in the south of Sweden and much of the wind capacity was assumed to be deployed in the north, adding the fact mentioned earlier, it is assumed that the 2 GW left to be allocated will be done so in zones SE3 and SE4. Therefore, the need for increased grid connection between zones is reduced and the chances of having prices differing so much between zones are also reduced.

Concerning hydropower plants, according to the PyPSA-Eur model, there are 145 hydropower plants scattered throughout Sweden yielding a total installed capacity of 14 GW, which is considerably lower than what was found in other sources [94]. Bearing in mind that the PyPSA-Eur model retrieves such data from openly available sources, sometimes the information may be incomplete or inaccurate. However, since there was not any data source with more complete information, the hydropower plants extracted from PyPSA-Eur were evenly scaled until meeting the current capacity of 16.3 GW [94].

The hourly hydropower energy generation at each node was assigned proportionally to the capacity at that same node. In other words, the installed hydro capacity weight at each node was calculated (installed hydro capacity at node divided by overall installed hydro capacity) and multiplied by the hourly hydropower generation in 2030 described in the previous section 4.5.3.

The electricity generation, regardless of the source, was at last assigned to a zone,

in other words, each transmission grid node was associated with a bidding zone and in turn its electricity generation as well.

4.5.5 Marginal costs of electricity generation sources

The electricity system model also requires that the marginal costs of available power plants are computed since they are required to run the electricity market model.

The marginal cost of electricity generation is given by the marginal cost of fuel plus the variable operations and maintenance costs [95]. The marginal fuel costs (FC), as well as variable operations and maintenance costs (VO&M) for the 6 different power generation sources, were retrieved from [96], [97], yielding the following marginal cost of electricity generation (MC) as it can be seen in Table 4.6. However, concerning hydropower plants, it was not possible to find variable operation and maintenance costs separate from annual O&M, hence the marginal cost was assumed to be 6 €/MWh as in [98].

Technology	[€/MWhth]	VOM [€/MWh]	MC [€/MWh]
Solar	-	0	0
Wind	-	0	0
Hydro	-	-	6
Nuclear	2	8	10
Biomass	-	-	32.5
Oil	50	3	53

Table 4.6: Marginal cost of the different electricity sources.

4.5.6 Electricity market model

The merit-order model was used to calculate the hourly electricity prices. The model aims to minimize the marginal generational costs, for each hour in each bidding zone. The constraints ensure that the electricity demand and supply are always met while taking into account the availability of electricity generation from the different sources.

From the previous sections, it is known that each bidding zone has an associated hourly load demand as well as generation from wind, solar and hydroelectric power. Besides, it also has an associated capacity from nuclear, biomass and fossil-based power plants as well as their respective marginal costs.

The market model can thus be written as the following optimisation problem. The objective is to minimize the generation costs.

$$\text{minimize} \quad \sum_s \lambda_s (g_{s_{SE1}} + g_{s_{SE2}} + g_{s_{SE3}} + g_{s_{SE4}})$$

$$\text{subject to} \quad d_{SE1} - \sum_s g_{s_{SE1}} = \Delta\delta_{SE1-SE2} : \lambda_{SE1}$$

$$d_{SE2} - \sum_s g_{s_{SE2}} = -\Delta\delta_{SE1-SE2} + \Delta\delta_{SE2-SE3} : \lambda_{SE2}$$

$$d_{SE3} - \sum_s g_{s_{SE3}} = -\Delta\delta_{SE2-SE3} + \Delta\delta_{SE3-SE4} : \lambda_{SE3}$$

$$d_{SE4} - \sum_s g_{s_{SE4}} = -\Delta\delta_{SE3-SE4} : \lambda_{SE4}$$

$$-8990 \leq \Delta\delta_{SE1-SE2} \leq 8990$$

$$-14580 \leq \Delta\delta_{SE2-SE3} \leq 14580$$

$$-12880 \leq \Delta\delta_{SE3-SE4} \leq 12880$$

Where,

λ_s stands for the marginal cost of the power source s.

$g_{s_{SE1}}$ stands for the generation of power source s, in zone $SE1$.

$g_{s_{SE2}}$ stands for the generation of power source s, in zone $SE2$.

$g_{s_{SE3}}$ stands for the generation of power source s, in zone $SE3$.

$g_{s_{SE4}}$ stands for the generation of power source s, in zone $SE4$.

λ_{SE1} stands for the electricity price in bidding zone SE1.

λ_{SE2} stands for the electricity price in bidding zone SE2.

λ_{SE3} stands for the electricity price in bidding zone SE3.

λ_{SE4} stands for the electricity price in bidding zone SE4.

$\Delta\delta_{SE1-SE2}$ stands for the transmission capacity between zones SE1 and SE2.

$\Delta\delta_{SE2-SE3}$ stands for the transmission capacity between zones SE2 and SE3.

$\Delta\delta_{SE3-SE4}$ stands for the transmission capacity between zones SE3 and SE4.

4.6 Sensitivity analysis

In order to understand the impacts of having major price differences between zones SE3, SE4 and SE2, prices in zones SE3 and SE4 were doubled. Regarding the centralised design, the objective of this sensitivity analysis is to understand how the optimisation of the electrolysers' locations will change as the HRS are located mainly in zones SE3 and SE4. Concerning the decentralised model, it is an interesting analysis to see how much more the overall supply chain cost will increase as the electrolysers are located at the same site as the HRSs. At last, this analysis is also quite interesting to see how it affects the mixed model, maybe in zones SE1 and SE2 production will be decentralised, whereas for HRS in zone SE3 and SE4 the electrolysers' facilities will be located in zone SE2.

Hydrogen demand was also increased in steps of 25% till 100% for the centralised design in gaseous state as the supply chain's cost was lower than in liquid state. The same sensitivity analysis was conducted for the decentralised design. The purpose of this sensitivity analysis is to investigate the impact of increasing the hydrogen demand on electricity prices and the supply chains' overall cost.

Chapter 5

Results

In the following section, the results will be presented, analysed and discussed. The structure of this section will begin with the electricity system, followed by the hydrogen supply chain design and back to the electricity system model exploring the feedback effects. The sensitivity analysis's results are also described in this section and a contribution to sustainability is presented at the end.

5.1 Electricity system model

After running the market model, the Swedish power mix for 2030 can be denoted and compared to the one in 2021 in Figure 5.1. It can be clearly denoted that hydro remained a major electricity generation source, alongside wind energy instead of nuclear as in 2021. In fact, the wind energy share grew from 17% to around 42%, whereas nuclear decreased from 30% to just 14%. Combined heat and power plants, which were mainly powered by bio-fuels, decreased from around 8% to less than 1%. Fossil fuels were not used at all. This means that by 2030, the Swedish electricity power industry should be almost fully decarbonised and provide green electricity as for the considered scenario in the study. Moreover, the average electricity price in €/MWh, is 4.28, 1.88, 8.21, 8.19 for zones SE1, SE2, SE3 and SE4, respectively. Furthermore, in 2030 the installed capacities, per source and per zone can be seen below. The total installed capacity is 57.1 GW, which is much higher than the roughly 42 GW installed in 2021 [88].
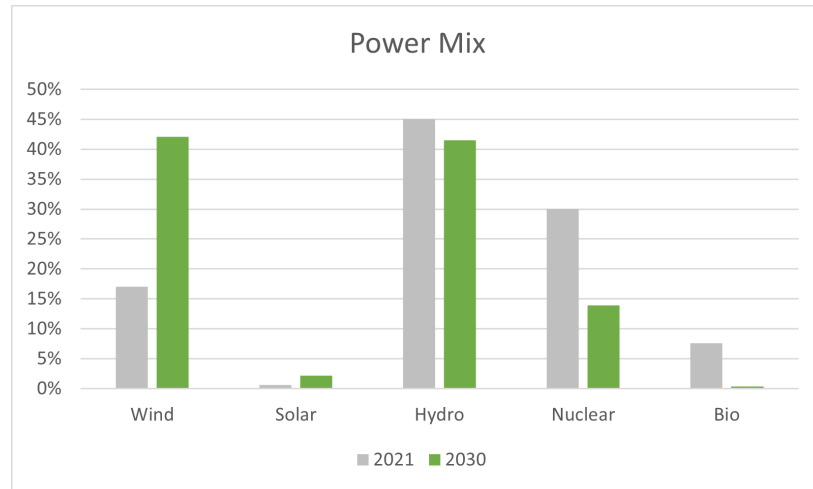
Figure 5.1: Swedish Power Mix in 2030 and 2021.
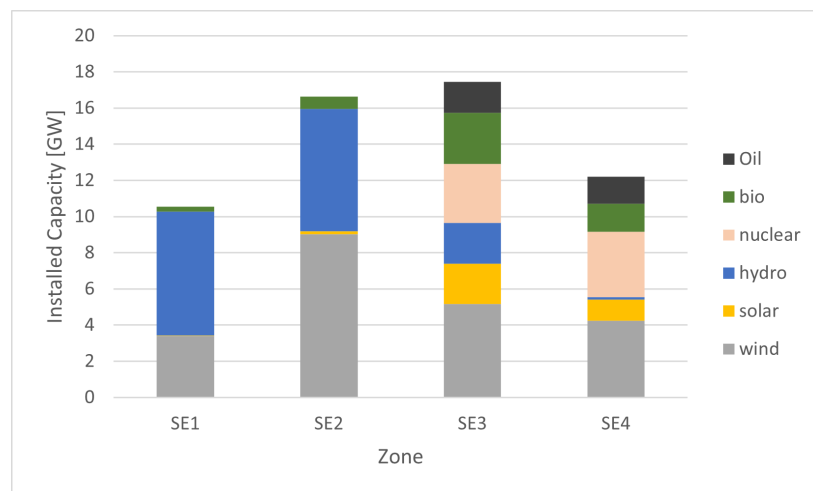
Figure 5.2: Installed capacity per source in each zone in 2030.

5.2 Hydrogen supply chain

The hydrogen models discussed in section methodolgy includes:

- the location of the HRSs.

- the optimized location of the electrolysers, in the case of the centralised models.

- their hourly hydrogen production rate, in other words, their capacity.

46

- the optimized transportation volume between each electrolyser and hydrogen fuel station, in the case of the centralised models.

- the resulting hydrogen price.

As mentioned, one of the inputs is the allocation of the HRSs, which can be seen in figure 5.3a. Figure 5.3b portrays a map with the location of 139 charging stations to be deployed in Sweden by autumn of 2023 the latest [99], [100]. It can be noted that there are significantly more charging stations in the South of Sweden, where there is a higher population density and many are located on highways. One could assume that as the FCEV technology matures and FCVEs increase the hydrogen refuelling infrastructure will develop following the charging infrastructure. By comparing both figures, it is possible to see that the allocation of the HRS performed by the hydrogen supply chain model is in accordance with such assumption.
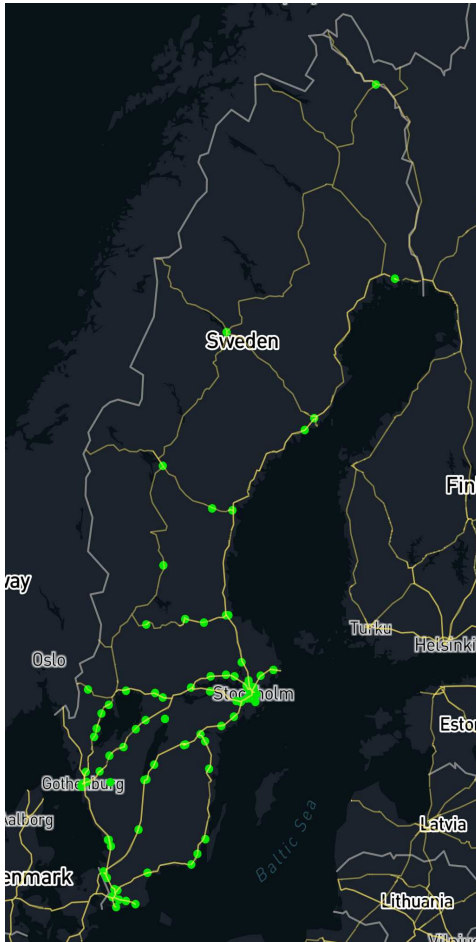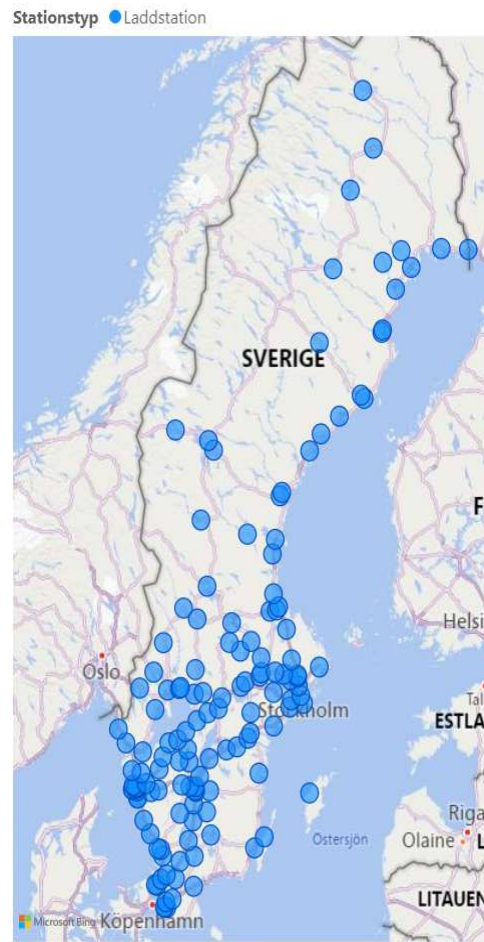
(a)   (b)

Figure 5.3: HRS allocation without seasonal variation. (a) Approved electric charging stations (b) [99], [100].

Tables 5.1 and 5.7 show the overall supply chain's cost, in $\text{€}/kg_{H_2}$, regarding every model and both scenarios, respectively, as in figure 4.2 [1]. As it can be seen from the pie charts from figure 5.4 to 5.9, the most significant costs are the production capital costs and the fuel station capital costs. The overall cost is higher in the centralised design than in the decentralised one. It can be denoted from the pie charts that this is due to transportation costs, and there are additional conversion costs in the case of the centralised LH_2 supply chain design. The centralised model in liquid state is always more expensive than in gaseous state due to conversion costs despite having lower transportation operational costs. There is no difference between the mixed models and the decentralised ones based on the designs used for the study, which means there is no advantage in having centralised production with the considered assumptions. The overall cost is higher in the scenario with seasonal variation as more hydrogen fuel stations were deployed to meet days with higher hydrogen demand which led to higher stations capital costs (SCC) and transportation capital costs (TCC). It is clear that increasing the number of HRS increases the stations' capital cost (SCC). The transportation capital costs increase as the model states that an HRS is supplied by only one truck. Furthermore, production capital costs and conversion capital costs increase as both the electrolysers and conversion facilities must have enough capacity to handle higher daily hydrogen demands than in the scenario without seasonal variation. It also possible to observe from pie charts in Figures 5.4, 5.5, 5.7 and 5.8, that regarding the centralised design, production capital costs are lower in gaseous state than in liquid state at the expense of leading to higher production operational costs.

Scenario	without seasonal variation			
Type	Centralised		Mixed	Decentralised
State	$H_2(g)$	$H_2(l)$	$H_2(g)$	$H_2(g)$
Price [€/kg]	2.00	2.63	1.48	1.48

Table 5.1: Hydrogen cost, in €/kg, for every model and scenario without seasonal variation.

Scenario	with seasonal variation			
Type	Centralised		Mixed	Decentralised
State	$H_2(g)$	$H_2(l)$	$H_2(g)$	$H_2(g)$
Price [€/kg]	2.29	3.13	1.68	1.68

Table 5.2: Hydrogen cost, in €/kg, for every model and scenario with seasonal variation.

---

[1]The centralised design was run with a mipgap of 15 %, whereas both decentralised and mixed designs with a mipgap of 1%.

Figure 5.4: Hydrogen cost component, in €/kg, regarding the centralised model without seasonal variation in gaseous state.

Figure 5.5: Hydrogen cost component, in €/kg, regarding the centralised model without seasonal variation in liquid state.

Figure 5.6: Hydrogen cost component, in €/kg, regarding the decentralised model without seasonal variation.
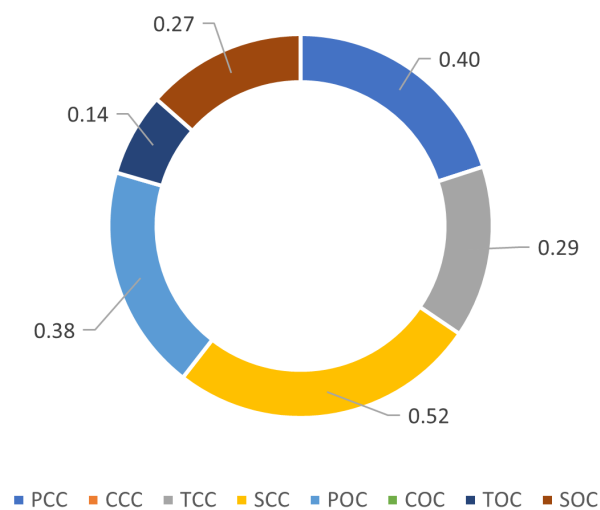

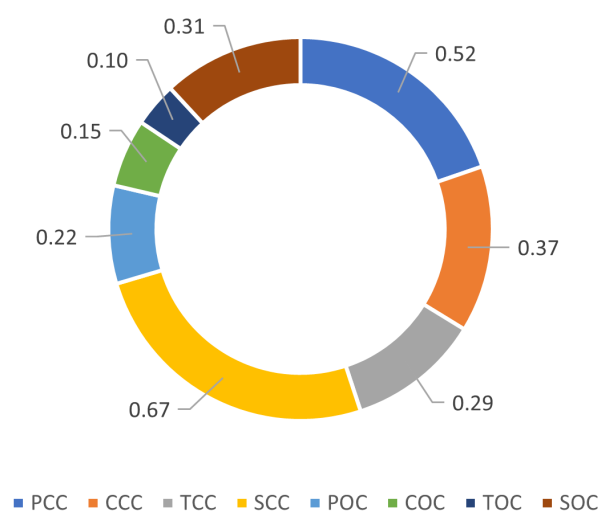Figure 5.7: Hydrogen cost component, in €/kg, regarding the centralised model with seasonal variation in gaseous state.
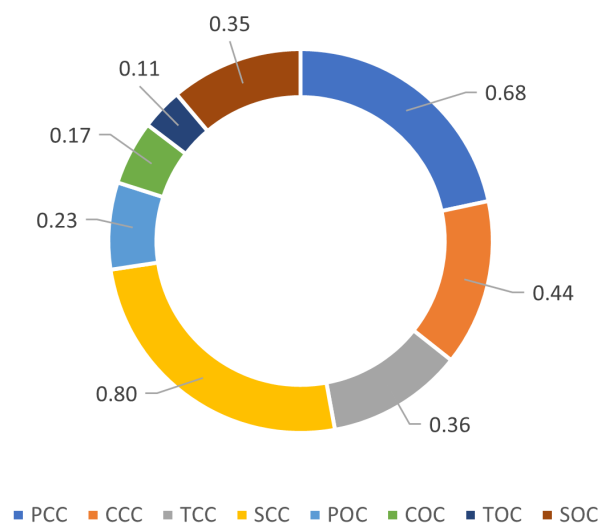
Figure 5.8: Hydrogen cost component, in €/kg, regarding the centralised model with seasonal variation in liquid state.
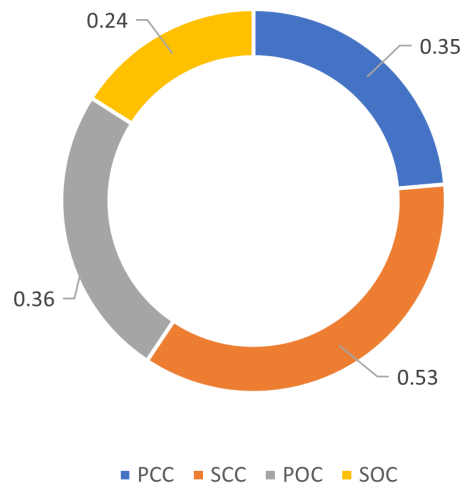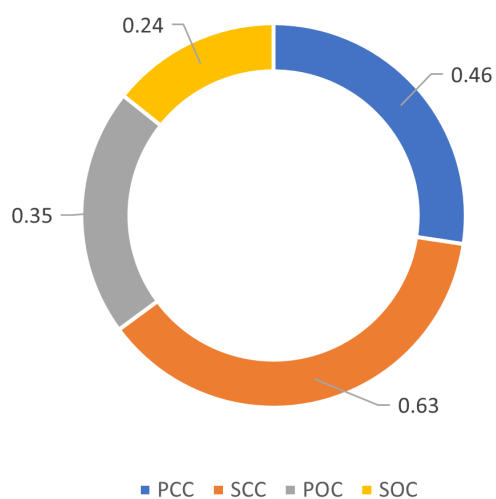

Figure 5.9: Hydrogen cost component, in €/kg, regarding the decentralised model with seasonal variation.

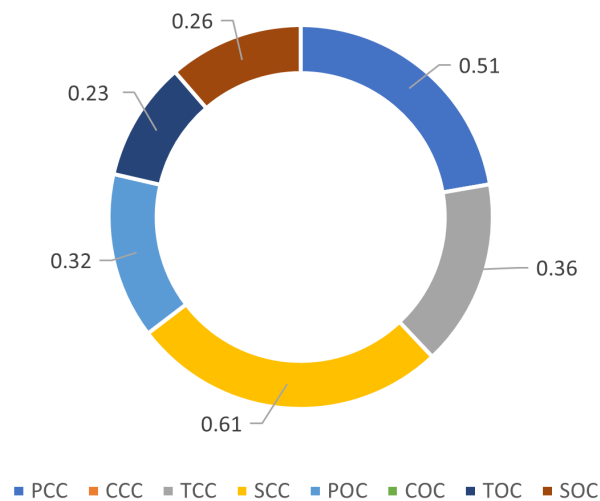Figures 5.10a and 5.10b depict the hydrogen supply chain infrastructure for the centralised design without seasonal variation. The white dots represent the electrolysers, the green dots represent the HRSs and the red lines the connections established. It can be observed from the figures that in the design in liquid state there are no electrolysers in zone SE3, contrary to the design in gaseous state. This can be explained due to lesser transportation operational costs as trailers carrying hydrogen in liquid state carry up to four times more hydrogen than trailers carrying hydrogen in gaseous state. Thus, it pays off to move more hydrogen production to zone SE2 where the electricity prices are lower.

Electrolysers that supply a greater number of HRSs are bigger in size than electrolysers that supply fewer HRSs. In figure 5.10b, it can be seen that two major electrolysers are located in SE2 and supply all the HRSs in SE3. The installed capacity of those two electrolysers is 99 MW and 22 MW. Furthermore, by analysing the hourly production data, it was possible to observe that having seasonal variation increased the electrolysis total installed capacity. In fact, in scenario without seasonal variation, the electrolysis total installed capacity was 190 MW and 249 MW for gaseous and liquid states respectively. Whereas in scenario with seasonal variation, electrolysis total installed capacity was 303 MW and 325 MW for gaseous and liquid states respectively. This increase can be explained since in both scenarios the annual hydrogen demand is the same, thus in scenario with seasonal variation, there are days with higher demand than in scenario without seasonal variation. Consequently, the electrolysis total installed capacity must be higher on those days than in scenario without seasonal variation.

In the decentralised design without seasonal variation, the size of the electrolysers was the same for every HRS, roughly 1.8 MW, and they were operational every hour. Regarding the decentralised model with seasonal variation, the electrolysers' installed capacities were also the same for every HRS, however, in this scenario, the installed capacity was slightly higher, roughly 2MW. Also, the electrolysers were not operational the entire time, in fact, the capacity factor was slightly above 78%. Moreover, concerning the centralised design in gaseous state without seasonal variation, the number of electrolysers was 16, with sizes ranging from 10 MW to 26 MW and a capacity factor of 100 %. Regarding the same design for the scenario with seasonal variation, the number of electrolysers was 18, with sizes ranging from 10 MW to 70 MW and a capacity factor ranging from 77% to 80%. Concerning the centralised design in liquid state, the electrolysers' sizes ranged from 10 MW to 99 MW with capacity factors from 70% to 80%, however, the number of electrolysers increased from 9 to 19 when seasonal variation was accounted for.

(a)   (b)
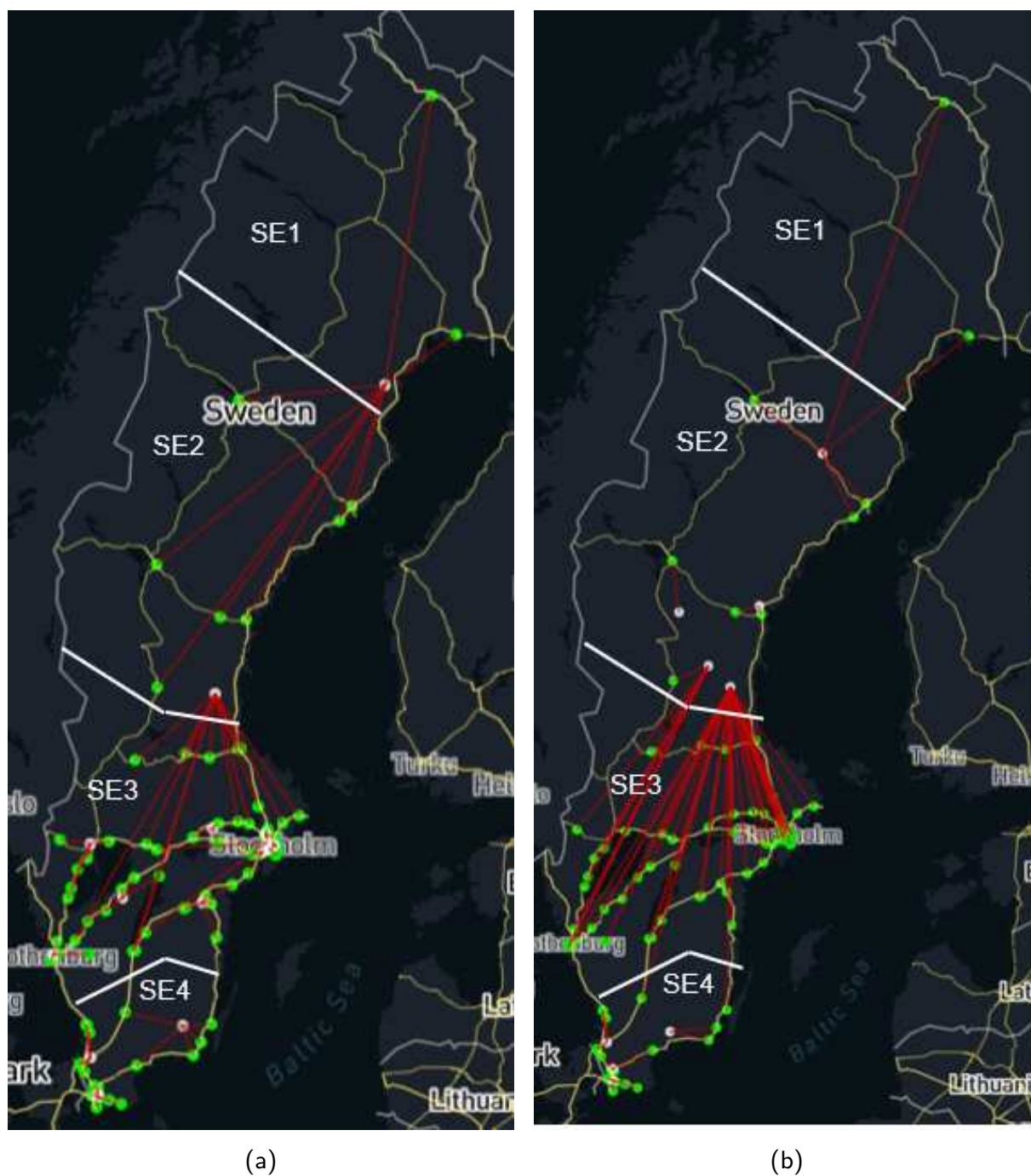
Figure 5.10: Electrolysers' locations and connections to the HRSs they supply - centralised design in gasesous state (a) and in liquid state (b) without seasonal variation.

5.3 Feedback Analysis - Electricity System

As mentioned in section 4, the hydrogen production prompted by the hydrogen models represents in fact an electricity demand. This extra electricity can have impacts on the electricity system, namely, driving prices higher. The goal of this subsection is to evaluate, quantitatively, the changes in the electricity system.

The feedback procedure mentioned in section 4.2.1 was conducted for every scenario and every model, excluding the mixed one as it was the same as the decentralised one, and the increase of the average prices can be seen in Tables 5.3 and 5.4. It can be concluded that hydrogen demand does have a significant impact on electricity prices. In addition, for the centralised model, the impact on the prices is mainly on zones SE2, SE3 and SE4, whereas, for the decentralised model the impact is mainly in zones SE3 and SE4, which makes sense since this is where most of the electrolysers are located.

scenario	without seasonal variation					
design	Centralized				Decentralized	
elec. price	$H_2(g)$		$H_2(l)$		$H_2(g)$	
SE1	4.28	4.37	2.10%	4.28	0.00%	4.31	0.70%
SE2	1.88	1.94	3.19%	2.34	24.47%	1.92	2.13%
SE3	8.21	8.40	2.31%	8.44	2.80%	8.36	1.83%
SE4	8.19	8.38	2.32%	8.42	2.81%	8.34	1.83%

Table 5.3: Increase of electricity price, in €/MWh, regarding scenario without seasonal variation.

scenario	with seasonal variation					
design	Centralized				Decentralized	
elec. price	$H_2(g)$		$H_2(l)$		$H_2(g)$	
SE1	4.28	4.41	3.04%	4.28	0.00%	4.32	0.93%
SE2	1.88	2.02	7.45%	2.35	25.00%	1.92	2.13%
SE3	8.21	8.49	3.41%	8.47	3.17%	8.37	1.95%
SE4	8.19	8.47	3.42%	8.45	3.17%	8.35	1.95%

Table 5.4: Increase of electricity price, in €/MWh, regarding scenario with seasonal variation.

5.4 Sensitivity Analysis Results

Concerning the centralised design in gaseous state, production operational costs decreased since more hydrogen was produced in zone SE2, which led to an increase in transportation operational costs. Regarding the centralised design in liquid state, the increase in the overall cost was mainly due to an increase in production operational costs from the electrolysers in zone SE4. Transportation operational costs remained the same. In short, the centralised design in gaseous state increased transportation costs (moved hydrogen production from SE3 to SE2) in order to decrease production operational costs and achieve a minimum overall cost. Since the centralised design in liquid sate had already most of its electrolysers located in SE2, which is the zone with lower electricity prices, transportation operational costs remained the same, however, production operational costs increased due to the electrolysers located in SE4. Table 5.5 shows the changes in costs due to the sensitivity analysis regarding the centralised design. These changes can be further analysed, concerning the centralised design in gaseous state, from figures 5.10a and 5.11a which show that the electrolysers located in SE3 no longer exist when the electricity prices are doubled in zones SE3 and SE4. In fact, the HRSs that were supplied by those electrolysers are now supplied by either one of the two electrolysers located above Stockholm, in zone SE2. Concerning the centralised design in liquid state without seasonal variation, no major difference can be seen between figures 5.10b and 5.11b.

	$H_2(g)$		$H_2(l)$	
	without sens. analysis	with sens. analysis	without sens. analysis	with sens. analysis
Sum	2.00	2.24	2.63	2.76
PCC	0.40	0.46	0.52	0.51
CCC	0.00	0.00	0.37	0.37
TCC	0.29	0.29	0.29	0.29
SCC	0.52	0.52	0.67	0.67
POC	0.38	0.35	0.22	0.32
COC	0.00	0.00	0.15	0.17
TOC	0.14	0.30	0.10	0.10
SOC	0.27	0.32	0.31	0.33

Table 5.5: Hydrogen supply chain cost changes regarding the centralised design, in €/kg_{H_2}, for the sensitivity analysis with doubled electricity prices in zones SE3 and SE4.

The same sensitivity analysis was also carried out for both the decentralised and mixed designs regarding scenario without seasonal variation. Contrary to the centralised design, the decentralised does not have the option to shift its production facilities to bidding zones with cheaper prices. Therefore, production operational costs increased much more than in the centralised design, actually doubling, leading to an increase in the overall cost of 0.36 $\text{€}/kg_{H_2}$, as can be seen in Table 5.6. Regarding the mixed design, it is quite interesting to observe that now there are transportation costs. This can be explained since with this difference in electricity prices, particularly between zones SE3 and SE2, it payed off to have some centralised production in zone SE2 supplying four HRSs in zone SE3.

	Decentralised		Mixed	
	without sens. analysis	with sens. analysis	without sens. analysis	with sens. analysis
Sum	1.48	1.83	1.48	1.83
PCC	0.35	0.35	0.35	0.54
CCC	0.00	0.00	0.00	0.00
TCC	0.00	0.00	0.00	0.04
SCC	0.53	0.53	0.53	0.52
POC	0.36	0.72	0.36	0.50
COC	0.00	0.00	0.00	0.00
TOC	0.00	0.00	0.00	0.01
SOC	0.24	0.24	0.24	0.23

Table 5.6: Hydrogen supply chain cost changes reagrding the decentralised and mixed designs, in $\text{€}/kg_{H_2}$, for the sensitivity analysis with doubled electricity prices in zones SE3 and SE4.

From this sensitivity analysis, it can be concluded that the centralised model is less sensitive to a scenario where the electricity prices in zones SE3 and SE4 are considerably higher than in zone SE2. The decentralised scenario is more sensitive since most of the HRSs are located in SE3 and SE4, hence this is also where the electrolysers are located.

(a)   (b)
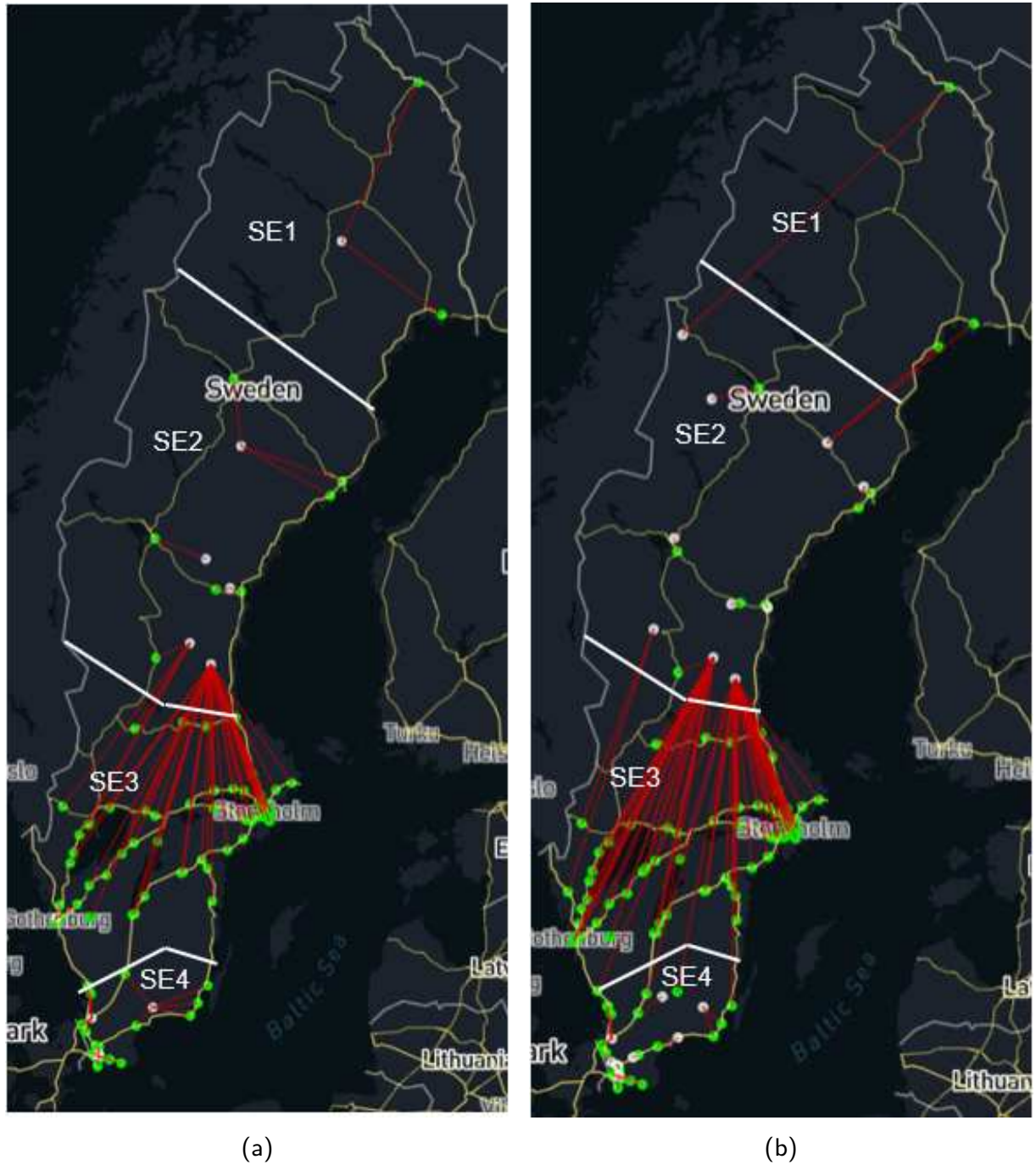
Figure 5.11: Electrolysers' locations and connections to the HRSs they supply, with doubled prices in SE3 and SE4 - centralised design in gasesous state (a) and in liquid state (b) without seasonal variation.

From tables 5.7 and 5.8 it is possible to conclude that by increasing the hydrogen demand the centralised supply chain's overall cost remains close to the base case. Whereas it can be seen in tables 5.9 and 5.10 that the decentralised supply chain's overall cost decreases steadily. This decrease is explained since there are learning effects in the capital cost of the fuel stations, thus, even though more fuel stations have to be deployed, the marginal cost decreases.

	$H_2(g)$ - without seasonal variation				
	0%	25%	50%	75%	100%
Sum	2.00	2.06	2.00	1.97	2.03
PCC	0.40	0.44	0.47	0.48	0.48
CCC	0.00	0.00	0.00	0.00	0.00
TCC	0.29	0.28	0.28	0.28	0.28
SCC	0.52	0.49	0.48	0.47	0.47
POC	0.38	0.33	0.39	0.37	0.41
COC	0.00	0.00	0.00	0.00	0.00
TOC	0.14	0.24	0.08	0.07	0.07
SOC	0.27	0.28	0.30	0.30	0.32

Table 5.7: Impact of increased hydrogen demand on the supply chain's overall cost, in €/kg_{H_2}, regarding the centralised design in gaseous state without seasonal variation.

	$H_2(g)$ - with seasonal variation				
	0%	25%	50%	75%	100%
Sum	2.29	2.29	2.20	2.20	2.22
PCC	0.51	0.51	0.51	0.55	0.55
CCC	0.00	0.00	0.00	0.00	0.00
TCC	0.36	0.36	0.35	0.36	0.36
SCC	0.61	0.61	0.59	0.58	0.58
POC	0.32	0.32	0.35	0.36	0.38
COC	0.00	0.00	0.00	0.00	0.00
TOC	0.23	0.23	0.14	0.06	0.06
SOC	0.26	0.26	0.26	0.29	0.29

Table 5.8: Impact of increased hydrogen demand on the supply chain's overall cost, in €/kg_{H_2}, regarding the centralised design gaseous state with seasonal variation.

	Decentralised without seasonal variation				
	0%	25%	50%	75%	100%
Sum	1.48	1.44	1.43	1.42	1.41
PCC	0.35	0.35	0.35	0.35	0.35
SCC	0.53	0.49	0.48	0.47	0.46
POC	0.36	0.36	0.37	0.37	0.36
SOC	0.24	0.24	0.24	0.24	0.24

Table 5.9: Impact of increased hydrogen demand on the supply chain's overall cost, in €/kg_{H_2}, regarding the decentralised design without seasonal variation.

	Decentralised with seasonal variation				
	0%	25%	50%	75%	100%
Sum	1.63	1.62	1.60	1.59	1.59
PCC	0.46	0.46	0.46	0.46	0.46
SCC	0.63	0.61	0.60	0.58	0.58
POC	0.32	0.32	0.32	0.32	0.32
SOC	0.22	0.22	0.22	0.22	0.22

Table 5.10: Impact of increased hydrogen demand on the supply chain's overall cost, in €/kg_{H_2}, regarding the decentralised design with seasonal variation.

As mentioned, in the centralised design in gaseous state, the electricity prices were mainly impacted on zones SE3 and SE4. Besides, in the decentralised design, the electrolysers are located in the same site as the HRSs, and since the vast majority are located in SE3 and SE4 that is where the highest electricity loads should occur. This conclusion can be confirmed in tables 5.13 and 5.14, as the prices in SE1 and SE2 only increase slightly, and prices in SE3 and SE4 increase much more.

		$H_2(g)$ - without seasonal variation				
	electricity price	0%	25%	50%	75%	100%
SE1	4.28	4.37	4.48	4.35	4.42	4.42
SE2	1.88	1.94	2.00	2.08	2.14	2.14
SE3	8.21	8.40	8.45	8.53	8.58	8.63
SE4	8.19	8.38	8.43	8.50	8.56	8.61

Table 5.11: Impact of increased hydrogen demand on the electricity prices, in €/MWh, regarding the centralised design in gaseous state without seasonal variation.

	electricity price	Decentralised without seasonal variation				
		0%	25%	50%	75%	100%
SE1	4.28	4.39	4.41	4.43	4.35	4.32
SE2	1.88	2.00	2.02	1.97	2.05	2.09
SE3	8.21	8.46	8.49	8.56	8.59	8.66
SE4	8.19	8.44	8.47	8.53	8.57	8.64

Table 5.12: Impact of increased hydrogen demand on the electricity prices, in $€/MWh$, regarding the centralised design in gaseous state with seasonal variation.

	electricity price	Decentralized without seasonal variation				
		0%	25%	50%	75%	100%
SE1	4.28	4.32	4.31	4.31	4.32	4.32
SE2	1.88	1.92	1.91	1.91	1.92	1.92
SE3	8.21	8.36	8.42	8.46	8.49	8.54
SE4	8.19	8.34	8.39	8.43	8.46	8.51

Table 5.13: Impact of increased hydrogen demand on the electricity prices, in $€/MWh$, regarding the decentralised design without seasonal variation.

	electricity price	Decentralized with seasonal variation				
		0%	25%	50%	75%	100%
SE1	4.28	4.31	4.30	4.31	4.32	4.31
SE2	1.88	1.92	1.90	1.90	1.91	1.92
SE3	8.21	8.37	8.37	8.40	8.50	8.46
SE4	8.19	8.35	8.34	8.37	8.47	8.43

Table 5.14: Impact of increased hydrogen demand on the electricity prices, in $€/MWh$, regarding the decentralised design with seasonal variation.

5.5   Limitations

There are some limitations in this work. Regarding the electricity system model, it does not portray:

- any type of cross-border power exchange.

- uncertainity of renewable energy sources and electricity demand.

- ramping up time of the generation sources as well as other technical specifications of the different technologies.

- changes in fuel costs.

- implementation of policies leading to changes in the marginal costs.

As can be observed, electricity prices are very low, which would change if the model included uncertainity from RES. The intraday market would be interesting to explore in order to see how the market would adjust to such changes. Furthermore, these limitations lead to nonexistent negative prices, which would be very interesting to incorporate, particularly for studying a hydrogen supply chain with storage.

Regarding the hydrogen model, including time-flexible operation improves the model's accuracy, however, at the expense of making it a more demanding optimisation problem that may require a computer with very high specifications. For the centralised and mixed designs, the optimisation was set to have an allowed gap of 15%. With such an allowed gap the centralised models usually took more than a day to run. In order to run the optimisations it was required to use a computer with an available RAM of 256 GB.

Furthermore, among the assumptions in the centralised design, it was assumed that the potential locations for electrolysers to be deployed were transmission grid substations. This assumption seems very reasonable as the electrolysers' size must be between 10 and 100 MW, which generates loads that require connection to large power transformers.

5.6 Contribution to sustainability

In order to tackle the current environmental crisis, it is urgent that all sectors reduce their greenhouse gas emissions substantially and swiftly. Alternative fuels, that do not release greenhouse gas emissions into the atmosphere, must replace fossil fuel transportation to achieve that goal.

FCEVs powered by hydrogen do not release greenhouse gas emissions, and if hydrogen is produced from renewable energy sources then the environmental impact of these vehicles becomes even more sustainable. As mentioned, the development of an adequate infrastructure is pivotal for the penetration of this technology.

By analysing different hydrogen supply chain designs and how they are intertwined with the electricity system, this study provides a methodology which showcases the cost minimal supply chain design according to the electricity system. Consequently, this study provides the necessary tools to efficiently plan the development of the FCEVs' infrastructure. This may prove to be crucial in the acceptance of FCEVs in Sweden and thus bring Sweden one step closer to its climate goals. Moreover, it also evaluates how the hydrogen supply chain impacts the electricity system.

Chapter 6

Conclusions

The average electricity prices in Sweden for zones SE1, SE2, SE3 and S4 are, in €/MWh, 4.28, 1.88, 8.21, 8.19 respectively. The electricity is mainly generated from wind and hydropower (around 42% each), followed by nuclear (14%), solar (2%) and then bioenergy (0.3%). The main changes in the power mix are the huge increase in wind power generation, the decrease in nuclear power generation, and particularly, the Swedish power mix is solely made up of RES as can be seen in Figure 5.1.

The hydrogen supply chain design that leads to a lower overall cost is the decentralised design, with a cost of 1.48 and 1.68 $€/kg_{H_2}$ concerning scenarios without and with seasonal variation respectively. It is cheapest by a margin of 0.52 and 0.61 $€/kg_{H_2}$ to the centralised design in gaseous state, in what concerns the scenario without and with seasonal variation, respectively. It is important to highlight that for the centralised design the achieved solution was just below 15% of the optimal solution, whereas for the decentralised design the solution was quite close to the optimal solution. Therefore, taking that into account, the difference between the optimal solutions is 0.30 and 0.36 $€/kg_{H_2}$, concerning scenarios without and with seasonal variation, respectively.

The scenario with seasonal variation leads to higher costs in the supply chain as more hydrogen fuel stations were deployed to meet days with higher hydrogen demand. This led to higher production capital costs (PCC) and fuel station capital costs (SCC) regarding every design, transportation capital costs (TCC) in the case of the centralised design, and conversion capital costs (CCC) in the case of the centralised design in liquid state.

It was also concluded that the centralised model is less sensitive to a scenario where the electricity prices in zones SE3 and SE4 are considerably higher than in zone SE2.

The decentralised scenario is more sensitive since most of the HRSs are located in SE4 and, particularly, SE3, thus the electrolysers as well. In addition, Increasing the hydrogen demand leads to a slightly lower supply chain overall cost concerning the decentralised design.

It can be concluded that hydrogen demand does have a significant impact on electricity prices. Furthermore, concerning the centralised model, the impact on the prices is mainly on zones SE2, SE3 and SE4, whereas, for the decentralised model the impact is mainly in zones SE3 and SE4, which makes sense since there is where most of the electrolysers are located. Moreover, the impact on the electricity prices from increasing the hydrogen demand is substantially more significant in the centralised model, which can be explained as the optimisation didn't achieve the optimal solution by 15% and thus resulted in unnecessary loads. As mentioned, in the centralised design, the hydrogen production was mainly focused on zone SE2, which is the one with the lowest electricity prices, and transported to the HRSs in the other zones. Besides, in the decentralised design, the electrolysers are located in the same site as the HRSs, and since the vast majority are located in SE3 and SE4 that is where the highest electricity occurred.

Concerning future work, the electricity system model should be broadened in order to reduce the current limitations and to allow studying the synergies between the hydrogen supply chain designs and the electricity system in more detail. The hydrogen supply chain could include storage, which could lead to reductions in the overall supply chain and in electricity redispacth costs (if comprehended in the electricity system model). For instance, including storage could allow demand flexibility solutions to be explored. Moreover, this study's approach provides great geographical granularity at the expense of considering Sweden as a closed system with no power or hydrogen exchanges with foreign entities. In other words, it does not comprehend the imports and exports of electricity or hydrogen. Geographic extension to a European scope could be interesting to model, however, it would need significant extra modelling effort.

Bibliography

[1] *The Paris Agreement*. [Online]. Available: https://unfccc.int/process-and-meetings/the-paris-agreement/the-paris-agreement.

[2] *A European Green Deal*. [Online]. Available: https://ec.europa.eu/info/strategy/priorities-2019-2024/european-green-deal_en.

[3] *How are emissions of greenhouse gases in the EU evolving?* [Online]. Available: https://ec.europa.eu/eurostat/cache/infographs/energy/bloc-4a.html?lang=en.

[4] *Greenhouse gas emissions from transport in Europe*. [Online]. Available: https://www.eea.europa.eu/ims/greenhouse-gas-emissions-from-transport.

[5] "World Energy Outlook 2021," en, p. 386,

[6] "Hitting the EV inflection point," Bloomberg New Energy Finance (BNEF), Tech. Rep., May 2021, p. 58. [Online]. Available: https://www.transportenvironment.org/wp-content/uploads/2021/08/2021_05_05_Electric_vehicle_price_parity_and_adoption_in_Europe_Final.pdf.

[7] T. Pollard, "Are hydrogen fuel-cell cars the future?," Jan. 2022. [Online]. Available: https://www.carmagazine.co.uk/electric/are-hydrogen-fuel-cell-cars-the-future/.

[8] S. Edelstein, "Battery electric or hydrogen fuel cell? VW lays out why one is the winner," Jan. 2020. [Online]. Available: https://www.greencarreports.com/news/1127660_battery-electric-or-hydrogen-fuel-cell-vw-lays-out-why-one-is-the-winner#:~:text=Put%20simply%2C%20batteries%20are%20far,chemical%20reaction%20in%20the%20cells.

[9] A. Ohnsman, "Batteries Or Hydrogen For Big (Clean) Trucks? Volvo Group Bets On Both," Feb. 2021. [Online]. Available: https://www.forbes.com/sites/alanohnsman/2021/03/02/batteries-or-hydrogen-for-big-clean-trucks-volvo-group-bets-on-both/?sh=2262dcea4371.

[10] *Nikola Two: Fuel-Cell Electric Sleeper Semi-Truck*. [Online]. Available: https://nikolamotor.com/two-fcev.

[11] *A climate smart solution for heavy transport Hydrogen fuel cells*. [Online]. Available: `https : / / www . volvogroup . com / en / future - of - transportation / innovation/electromobility/hydrogen-fuel-cells.html`.

[12] *SVERIGES NATIONELLA STATISTIK FÖR ELBILAR OCH LADDINFRASTRUK-TUR*. [Online]. Available: `https://www.elbilsstatistik.se/`.

[13] *Hydrogen as a fuel for fuel cell electric vehicles*. [Online]. Available: `https :// www.ieafuelcell.com/index.php?id=33`.

[14] S. Herbst and J. Guldner, "The path to net zero: Deploying both battery and fuel cell electric vehicles," *Innovation News Network*, Jul. 2022. [Online]. Available: `https : / / www . innovationnewsnetwork . com / net - zero - battery - fuel - cell-electric-vehicles/21185/`.

[15] C. Brooks, "Germany leads pack of countries pouring finance into hydrogen," [Online]. Available: `https://cleanenergynews.ihsmarkit.com/research- analysis / germany - tops - table - of - states - pouring - finance - into - hydrogen . html# : ~ : text = The % 20firm % 20looked % 20at % 20state , and % 20planned%20hydrogen%20production%20capacity.`.

[16] G. Cipriani, V. D. Dio, F. Genduso, *et al.*, "Perspective on hydrogen energy carrier and its automotive applications," *International Journal of Hydrogen Energy*, vol. 39, no. 16, pp. 8482–8494, 2014, ISSN: 0360-3199. DOI: `https : / / doi . org/10.1016/j.ijhydene.2014.03.174`. [Online]. Available: `https://www. sciencedirect.com/science/article/pii/S0360319914008660`.

[17] *Hydrogen and Fuel Cell Technologies Office Multi-Year Research, Development, and Demonstration Plan*, Oct. 2014. [Online]. Available: `https://www.energy. gov/eere/fuelcells/articles/hydrogen-and-fuel-cell-technologies- office-multi-year-research-development`.

[18] C. Yang and J. Ogden, "Determining the lowest-cost hydrogen delivery mode," *International Journal of Hydrogen Energy*, vol. 32, no. 2, pp. 268–286, 2007, ISSN: 0360-3199. DOI: `https://doi.org/10.1016/j.ijhydene.2006.05.009`. [Online]. Available: `https://www.sciencedirect.com/science/article/ pii/S0360319906001765`.

[19] K. Reddi, A. Elgowainy, D. Brown, N. Rustagi, M. Mintz, and J. Gillete, "Hydrogen delivery scenario analysis model," *Department of Energy (DOE): Oak Ridge, TN, USA*, 2015.

[20] M. Reuß, T. Grube, M. Robinius, P. Preuster, P. Wasserscheid, and D. Stolten, "Seasonal storage and alternative carriers: A flexible hydrogen supply chain model," en, *Applied Energy*, vol. 200, pp. 290–302, Aug. 2017, ISSN: 03062619. DOI: `10. 1016/j.apenergy.2017.05.050`. [Online]. Available: `https://linkinghub. elsevier.com/retrieve/pii/S0306261917305457` (visited on 07/19/2022).

[21]   S. Schiebahn, T. Grube, M. Robinius, V. Tietze, B. Kumar, and D. Stolten, "Power to gas: Technological overview, systems analysis and economic assessment for a case study in Germany," en, *International Journal of Hydrogen Energy*, vol. 40, no. 12, pp. 4285–4294, Apr. 2015, ISSN: 03603199. DOI: `10.1016/j.ijhydene.2015.01.123`. [Online]. Available: `https://linkinghub.elsevier.com/retrieve/pii/S0360319915001913` (visited on 07/02/2022).

[22]   N. Popovich, "2015 Annual Progress Report: DOE Hydrogen and Fuel Cells Program," Dec. 2015. [Online]. Available: `https://www.osti.gov/biblio/1233740`.

[23]   M. Gardiner, "Energy requirements for hydrogen gas compression and liquefaction as related to vehicle storage needs," *DOE hydrogen and fuel cells program record*, vol. 9013, 2009, Publisher: DOE Washington, DC, USA.

[24]   "Running on hydrogen thanks to COPERNIC," Sep. 2018. [Online]. Available: `https://www.cea.fr/english/Pages/News/Running-on-hydrogen-thanks-to-COPERNIC.aspx`.

[25]   S. Niaz, T. Manzoor, and A. H. Pandith, "Hydrogen storage: Materials, methods and perspectives," *Renewable and Sustainable Energy Reviews*, vol. 50, pp. 457–469, 2015, ISSN: 1364-0321. DOI: `https://doi.org/10.1016/j.rser.2015.05.011`. [Online]. Available: `https://www.sciencedirect.com/science/article/pii/S1364032115004694`.

[26]   T.-P. Chen, "Hydrogen delivey infrastructure option analysis," Nexant, Inc., 101 2nd St., San Fancisco, CA 94105, Tech. Rep., 2010.

[27]   D. Teichmann, W. Arlt, and P. Wasserscheid, "Liquid Organic Hydrogen Carriers as an efficient vector for the transport and storage of renewable energy," *International Journal of Hydrogen Energy*, vol. 37, no. 23, pp. 18 118–18 132, 2012, ISSN: 0360-3199. DOI: `https://doi.org/10.1016/j.ijhydene.2012.08.066`. [Online]. Available: `https://www.sciencedirect.com/science/article/pii/S036031991201868X`.

[28]   D. Teichmann, W. Arlt, P. Wasserscheid, and R. Freymann, "A future energy supply based on Liquid Organic Hydrogen Carriers (LOHC)," *Energy Environ. Sci.*, vol. 4, no. 8, pp. 2767–2773, 2011, Publisher: The Royal Society of Chemistry. DOI: `10.1039/C1EE01454D`. [Online]. Available: `http://dx.doi.org/10.1039/C1EE01454D`.

[29]   H. Dagdougui, "Models, methods and approaches for the planning and design of the future hydrogen supply chain," *International Journal of Hydrogen Energy*, vol. 37, no. 6, pp. 5318–5327, 2012, ISSN: 0360-3199. DOI: `https://doi.org/10.1016/j.ijhydene.2011.08.041`. [Online]. Available: `https://www.sciencedirect.com/science/article/pii/S0360319911019288`.

[30] M. Reuß, T. Grube, M. Robinius, and D. Stolten, "A hydrogen supply chain with spatial resolution: Comparative analysis of infrastructure technologies in Germany," en, *Applied Energy*, vol. 247, pp. 438–453, Aug. 2019, ISSN: 03062619. DOI: 10.1016/j.apenergy.2019.04.064. [Online]. Available: https://linkinghub.elsevier.com/retrieve/pii/S0306261919307111 (visited on 07/02/2022).

[31] P. Bolat and C. Thiel, "Hydrogen supply chain architecture for bottom-up energy systems models. Part 1: Developing pathways," *International Journal of Hydrogen Energy*, vol. 39, no. 17, pp. 8881–8897, 2014, ISSN: 0360-3199. DOI: https://doi.org/10.1016/j.ijhydene.2014.03.176. [Online]. Available: https://www.sciencedirect.com/science/article/pii/S0360319914008684.

[32] P. Bolat and C. Thiel, "Hydrogen supply chain architecture for bottom-up energy systems models. Part 2: Techno-economic inputs for hydrogen production pathways," *International Journal of Hydrogen Energy*, vol. 39, no. 17, pp. 8898–8925, 2014, ISSN: 0360-3199. DOI: https://doi.org/10.1016/j.ijhydene.2014.03.170. [Online]. Available: https://www.sciencedirect.com/science/article/pii/S0360319914008623.

[33] P. Seydel, "Entwicklung und Bewertung einer langfristigen regionalen Strategie zum Aufbau einer Wasserstoffinfrastruktur-auf Basis der Modellverknüpfung eines Geografischen Informationssystems und eines Energiesystemmodells," PhD Thesis, ETH Zurich, 2008.

[34] D. Krieg, *Konzept und Kosten eines Pipelinesystems zur Versorgung des deutschen Straßenverkehrs mit Wasserstoff*. Forschungszentrum Jülich, 2012, vol. 144.

[35] S. Baufumé, F. Grüger, T. Grube, *et al.*, "GIS-based scenario calculations for a nationwide German hydrogen pipeline infrastructure," *International Journal of Hydrogen Energy*, vol. 38, no. 10, pp. 3813–3829, 2013, ISSN: 0360-3199. DOI: https://doi.org/10.1016/j.ijhydene.2012.12.147. [Online]. Available: https://www.sciencedirect.com/science/article/pii/S0360319913000670.

[36] M. Robinius, A. Otto, P. Heuser, *et al.*, "Linking the Power and Transport Sectors—Part 1: The Principle of Sector Coupling," *Energies*, vol. 10, no. 7, 2017, ISSN: 1996-1073. DOI: 10.3390/en10070956. [Online]. Available: https://www.mdpi.com/1996-1073/10/7/956.

[37] M. Robinius, A. Otto, K. Syranidis, *et al.*, "Linking the Power and Transport Sectors—Part 2: Modelling a Sector Coupling Scenario for Germany," *Energies*, vol. 10, no. 7, 2017, ISSN: 1996-1073. DOI: 10.3390/en10070957. [Online]. Available: https://www.mdpi.com/1996-1073/10/7/957.

[38] M. Moreno-Benito, P. Agnolucci, and L. G. Papageorgiou, "Towards a sustainable hydrogen economy: Optimisation-based framework for hydrogen infrastructure development," *Computers & Chemical Engineering*, vol. 102, pp. 110–127, 2017, ISSN: 0098-1354. DOI: `https://doi.org/10.1016/j.compchemeng.2016.08.005`. [Online]. Available: `https://www.sciencedirect.com/science/article/pii/S0098135416302666`.

[39] A. Almansoori and A. Betancourt-Torcat, "Design of optimization model for a hydrogen supply chain under emission constraints - A case study of Germany," *Energy*, vol. 111, pp. 414–429, 2016, ISSN: 0360-5442. DOI: `https://doi.org/10.1016/j.energy.2016.05.123`. [Online]. Available: `https://www.sciencedirect.com/science/article/pii/S0360544216307514`.

[40] S. Samsatli, I. Staffell, and N. J. Samsatli, "Optimal design and operation of integrated wind-hydrogen-electricity networks for decarbonising the domestic transport sector in Great Britain," *international journal of hydrogen energy*, vol. 41, no. 1, pp. 447–475, 2016, Publisher: Elsevier.

[41] L. Welder, D. S. Ryberg, L. Kotzur, T. Grube, M. Robinius, and D. Stolten, "Spatio-temporal optimization of a future energy system for power-to-hydrogen applications in Germany," *Energy*, vol. 158, pp. 1130–1149, 2018, Publisher: Elsevier.

[42] A. O. Bique and E. Zondervan, "An outlook towards hydrogen supply chain networks in 2050 — Design of novel fuel infrastructures in Germany," *Chemical Engineering Research and Design*, vol. 134, pp. 90–103, 2018, ISSN: 0263-8762. DOI: `https://doi.org/10.1016/j.cherd.2018.03.037`. [Online]. Available: `https://www.sciencedirect.com/science/article/pii/S0263876218301643`.

[43] M. Yáñez, A. Ortiz, B. Brunaud, I. E. Grossmann, and I. Ortiz, "Contribution of upcycling surplus hydrogen to design a sustainable supply chain: The case study of Northern Spain," *Applied Energy*, vol. 231, pp. 777–787, 2018, ISSN: 0306-2619. DOI: `https://doi.org/10.1016/j.apenergy.2018.09.047`. [Online]. Available: `https://www.sciencedirect.com/science/article/pii/S0306261918313564`.

[44] S. D.-L. Almaraz, C. Azzaro-Pantel, L. Montastruc, and S. Domenech, "Hydrogen supply chain optimization for deployment scenarios in the Midi-Pyrénées region, France," *International Journal of Hydrogen Energy*, vol. 39, no. 23, pp. 11 831–11 845, 2014, ISSN: 0360-3199. DOI: `https://doi.org/10.1016/j.ijhydene.2014.05.165`. [Online]. Available: `https://www.sciencedirect.com/science/article/pii/S0360319914015778`.

[45] S. D.-L. Almaraz, C. Azzaro-Pantel, L. Montastruc, L. Pibouleau, and O. B. Senties, "Assessment of mono and multi-objective optimization to design a hydrogen supply chain," *International Journal of Hydrogen Energy*, vol. 38, no. 33, pp. 14 121–14 145, 2013, ISSN: 0360-3199. DOI: `https://doi.org/10.1016/j.ijhydene.2013.07.059`. [Online]. Available: `https://www.sciencedirect.com/science/article/pii/S0360319913018065`.

[46] J. André, S. Auray, J. Brac, *et al.*, "Design and dimensioning of hydrogen transmission pipeline networks," *European Journal of Operational Research*, vol. 229, no. 1, pp. 239–251, 2013, ISSN: 0377-2217. DOI: `https://doi.org/10.1016/j.ejor.2013.02.036`. [Online]. Available: `https://www.sciencedirect.com/science/article/pii/S0377221713001690`.

[47] J. André, S. Auray, D. D. Wolf, M.-M. Memmah, and A. Simonnet, "Time development of new hydrogen transmission pipeline networks for France," *International Journal of Hydrogen Energy*, vol. 39, no. 20, pp. 10 323–10 337, 2014, ISSN: 0360-3199. DOI: `https://doi.org/10.1016/j.ijhydene.2014.04.190`. [Online]. Available: `https://www.sciencedirect.com/science/article/pii/S0360319914012804`.

[48] J. R. Centre, I. f. Energy, Transport, H. Maas, H. Hass, and A. Huss, *Well-to-wheels analysis of future automotive fuels and powertrains in the European context : tank-to-wheels report (TTW), version 4a, April 2014*, A. Krasenbrink, R. Edwards, L. Lonza, *et al.*, Eds. Publications Office, 2014. DOI: `doi/10.2790/95839`.

[49] A. Reid, R. Nelson, S. Godwin, *et al.*, *Well-to-tank report version 4.0 JEC well-to-wheels analysis: well-to-wheels analysis of future automotive fuels and powertrains in the European context.* en. Luxembourg: Publications Office, 2013, OCLC: 1044400677.

[50] A. (N. Laboratory), *Hydrogen Delivery Scenario Analysis Model (HDSAM) V3.0*, 2016.

[51] A. (N. Laboratory), *Hydrogen Refueling Station Analysis Model (HRSAM) V1.1*, 2016.

[52] D. Teichmann, *Konzeption und Bewertung einer nachhaltigen Energieversorgung auf Basis flüssiger Wasserstoffträgermaterialien (LOHC)*. Shaker, 2015.

[53] S. Moroz, X. F. Tan, J. Pierce, *et al.*, "Systems based on hypo-eutectic Mg–Mg2Ni alloys for medium to large scale hydrogen storage and delivery," *Journal of Alloys and Compounds*, vol. 580, S329–S332, 2013, ISSN: 0925-8388. DOI: `https://doi.org/10.1016/j.jallcom.2013.03.127`. [Online]. Available: `https://www.sciencedirect.com/science/article/pii/S0925838813006580`.

[54] C. Wulf, M. Reuß, T. Grube, *et al.*, "Life Cycle Assessment of hydrogen transport and distribution options," *Journal of Cleaner Production*, vol. 199, pp. 431–443, 2018, ISSN: 0959-6526. DOI: `https://doi.org/10.1016/j.jclepro.2018.07.180`. [Online]. Available: `https://www.sciencedirect.com/science/article/pii/S095965261832170X`.

[55] F. Vom Scheidt, J. Qu, P. Staudt, D. Mallapragada, and C. Weinhardt, "The effects of electricity tariffs on cost-minimal hydrogen supply chains and their impact on electricity prices and redispatch costs," en, 2021. DOI: `10.24251/HICSS.2021.401`. [Online]. Available: `http://hdl.handle.net/10125/71016` (visited on 02/18/2022).

[56] S. ANDERSSON and A. SÖRMAN, "Hydrogen System for Heavy Vehicles in Sweden Roles, Actors and Pathways for a Hydrogen Refueling Infrastructure," Ph.D. dissertation, CHALMERS UNIVERSITY OF TECHNOLOGY, Gothenburg, Sweden, Jun. 2021. [Online]. Available: `https://odr.chalmers.se/bitstream/20.500.12380/302510/1/E2021_029.pdf` (visited on 02/18/2022).

[57] D. G. Caglayan, N. Weber, H. U. Heinrichs, *et al.*, "Technical potential of salt caverns for hydrogen storage in Europe," *International Journal of Hydrogen Energy*, vol. 45, no. 11, pp. 6793–6805, 2020, ISSN: 0360-3199. DOI: `https://doi.org/10.1016/j.ijhydene.2019.12.161`. [Online]. Available: `https://www.sciencedirect.com/science/article/pii/S0360319919347299`.

[58] J. Cihlar, D. Mavins, and K. van der Leun, "Picturing the value of underground gas storage to the European hydrogen system," Gas Infrastructure Europe, Tech. Rep., Jun. 2021.

[59] G. Glenk and S. Reichelstein, "Economics of converting renewable power to hydrogen," en, *Nature Energy*, vol. 4, no. 3, pp. 216–222, Mar. 2019, ISSN: 2058-7546. DOI: `10.1038/s41560-019-0326-1`. [Online]. Available: `http://www.nature.com/articles/s41560-019-0326-1` (visited on 10/02/2022).

[60] M. E. Reuß, A. Moser, and D. Stolten, "Techno-ökonomische Analyse alternativer Wasserstoffinfrastruktur," Lehrstuhl für Brennstoffzellen (FZ Jülich), Tech. Rep., 2019.

[61] R. Hancke, T. Holm, and Ø. Ulleberg, "The case for high-pressure PEM water electrolysis," *Energy Conversion and Management*, vol. 261, p. 115 642, 2022, ISSN: 0196-8904. DOI: `https://doi.org/10.1016/j.enconman.2022.115642`. [Online]. Available: `https://www.sciencedirect.com/science/article/pii/S0196890422004381`.

[62] "Opportunities for Hydrogen Energy Technologies Considering the National Energy & Climate Plans," Fuel Cells and Hydrogen 2 Joint Undertaking (FCH 2 JU), Tech. Rep., 2020, p. 13. [Online]. Available: `https://www.fch.europa.eu/publications/opportunities-hydrogen-energy-technologies-considering-national-energy-climate-plans` (visited on 05/05/2022).

[63] T. Grube and D. Stolten, "The Impact of Drive Cycles and Auxiliary Power on Passenger Car Fuel Economy," en, *Energies*, vol. 11, no. 4, p. 1010, Apr. 2018, ISSN: 1996-1073. DOI: 10.3390/en11041010. [Online]. Available: `http://www.mdpi.com/1996-1073/11/4/1010` (visited on 07/02/2022).

[64] *Fuel Cell Heavy Duty Trucks Already In Service And Providing Many CO2 Emission-Free Kilometers*, Apr. 2019. [Online]. Available: `https://fuelcellsworks.com/news/fuel-cell-heavy-duty-trucks-already-in-service-and-providing-many-co2-emission-free-kilometers/` (visited on 05/17/2022).

[65] *Vehicles kilometres for Swedish road vehicles*, Apr. 2022. [Online]. Available: `https://www.scb.se/en/finding-statistics/statistics-by-subject-area/transport-and-communications/road-traffic/vehicles-kilometres-for-swedish-road-vehicles/` (visited on 04/25/2022).

[66] J. Vepsäläinen, K. Otto, A. Lajunen, and K. Tammi, "Computationally efficient model for energy demand prediction of electric city bus in varying operating conditions," *Energy*, vol. 169, pp. 433–443, 2019, ISSN: 0360-5442. DOI: `https://doi.org/10.1016/j.energy.2018.12.064`. [Online]. Available: `https://www.sciencedirect.com/science/article/pii/S0360544218324307`.

[67] M. I. R. Jacob, "Optimization of infrastructure investment for decarbonization of public buses through electricity and hydrogen," en, p. 98,

[68] *Ladda ner meteorologiska observationer - örebro Flygplats — SMHI.* [Online]. Available: `https://www.smhi.se/data/meteorologi/ladda-ner-meteorologiska-observationer/#param=airtemperatureInstant,stations=all,stationid=95130`.

[69] "A hydrogen strategy for a climate-neutral Europe," EUROPEAN COMMISSION, Tech. Rep., Aug. 2020, p. 24. [Online]. Available: `https://www.google.com/search?q=European+Commission%2C+%E2%80%9CA+hydrogen+strategy+for+a+climate-neutral+europe%2C%E2%80%9D+2020.&oq=European+Commission%2C+%E2%80%9CA+hydrogen+strategy+for+a+climate-neutral+europe%2C%E2%80%9D+2020.&aqs=chrome..69i57j0i22i30l3.789j0j7&sourceid=chrome&ie=UTF-8` (visited on 04/03/2022).

[70] T. Smolinka, M. Gunther, and J. Garche, ""NOW-Studie: ¨ Stand und Entwicklungspotenzial der Wasserelektrolyse zur Herstellung von Waserstoff aus regenerativen Energien," Tech. Rep., 2011.

[71] T. Young, *PEM electrolyser technology gaining favour*, Aug. 2022. [Online]. Available: `https://pemedianetwork.com/hydrogen-economist/articles/green-hydrogen/2022/pem-electrolyser-technology-gaining-favour/`.

[72] E. Bellini, "Large scale alkaline electrolyzers may be built at €444/kW in 2030," Sep. 2022. [Online]. Available: `https://www.pv-magazine.com/2022/02/09/large-scale-alkaline-electrolyzers-may-be-built-at-e444-kw-in-`.

[73] *Heavy Truck Driver*, Feb. 2022. [Online]. Available: `https://www.salaryexpert.com/salary/job/heavy-truck-driver/sweden`.

[74] "System Development Plan 2022–2031," en, p. 49, Nov. 2021. [Online]. Available: `https://www.svk.se/siteassets/om-oss/rapporter/2021/svk_systemutvecklingsplan_2022-2031_eng.pdf` (visited on 05/12/2022).

[75] *Grid Map*. [Online]. Available: `https://www.entsoe.eu/data/map/`.

[76] J. Egerer, "Data Documentation 83 Open source Electricity Model for Germany," en, p. 47,

[77] F. Kießling, P. Nefzger, and U. Kaintzyk, *Freileitungen: Planung, Berechnung, Ausfuhrung*. Springer-Verlag, 2011.

[78] *Transparency Platform*, 2018. [Online]. Available: `https:%20//tyndp.entsoe.eu/maps-data` (visited on 05/14/2021).

[79] F. vom Scheidt, C. Muller, P. Staudt, and C. Weinhardt, *The German Electricity System in 2030 - Data on Consumption, Generation, and the Grid*, 2020. [Online]. Available: `https://bwdatadiss.kit.edu/dataitem/download/4959` (visited on 02/14/2022).

[80] F. Todd, "Renewable energy capacity in Sweden to double to 30GW by 2030, says analyst," Jul. 2019. [Online]. Available: `https://www.nsenergybusiness.com/news/renewable-capacity-sweden-2030/` (visited on 05/20/2022).

[81] J. Fernando, "Compound Annual Growth Rate (CAGR)," English, Oct. 2021. [Online]. Available: `https://www.investopedia.com/terms/c/cagr.asp#:~:text=To%20calculate%20the%20CAGR%20of,one%20from%20the%20subsequent%20result.` (visited on 05/20/2022).

[82] "Statistics and forecast 2021 – Q2," English, SWEA, Swedish Wind Energy Association - Svensk Vindenergi, Tech. Rep., Jul. 2021, p. 15. [Online]. Available: `https://svenskvindenergi.org/wp-content/uploads/2021/06/Q2-2021-Statistics-and-forecast-Svensk-Vindenergi-210701_FINAL.pdf` (visited on 05/20/2022).

[83] E. Bellini, "Sweden hits 1 GW milestone," Jan. 2021. [Online]. Available: `https://www.pv-magazine.com/2021/04/01/sweden-hits-1-gw-milestone/#:~:text=Sweden's%20operational%20PV%20capacity%20increased,from%20the%20Swedish%20Energy%20Agency.` (visited on 05/20/2022).

[84] *Svensk Solenergi - Statistik*, Swedish. [Online]. Available: `https://svensksolenergi.se/statistik/solkraft/` (visited on 05/21/0202).

[85] *Actual Generation per Production Type*. [Online]. Available: `https://transparency.entsoe.eu/generation/r2/actualGenerationPerProductionType/show` (visited on 05/20/2022).

[86] *Facts about Swedish wind energy*, Jun. 2021. [Online]. Available: `https : / / nordic . baywa - re . com / en / wind / wind - facts - sweden# : ~ : text = In % 202014 % 20the % 20average % 20capacity , a % 20capacity % 20factor % 20of % 2037 % 25`. (visited on 05/20/2022).

[87] *PVGIS Photovoltaic Geographical Information System*. [Online]. Available: `https : //joint-research-centre.ec.europa.eu/pvgis-photovoltaic-geographical- information-system_en` (visited on 05/21/2022).

[88] "Energy in Sweden – An overview," en, Energimyndigheten - Swedish Energy Agency, Tech. Rep., p. 18. [Online]. Available: `https://energimyndigheten. a-w2m.se/Home.mvc?ResourceId=198022`.

[89] E. Jangö, "Kraftbalansen på den svenska elmarknaden, rapport 2022," sv, p. 67, 2022. [Online]. Available: `https : / / www . svk . se / siteassets / om - oss / rapporter/2022/kraftbalansen-pa-den-svenska-elmarknaden-rapport- 2022.pdf`.

[90] *Energy use in Sweden*, Jul. 2021. [Online]. Available: `https : // sweden . se / climate/sustainability/energy-use-in-sweden` (visited on 05/20/2022).

[91] "Systemutvecklingsplan 2022–2031," sv, p. 193, [Online]. Available: `https : // www.svk.se/systemutvecklingsplan`.

[92] *Nätanslutna solcellsanläggningar*. [Online]. Available: `https : / / pxexternal . energimyndigheten.se/pxweb/sv/N%C3%A4tanslutna%20solcellsanl%C3% A4ggningar/N%C3%A4tanslutna%20solcellsanl%C3%A4ggningar/?rxid= 5e71cfb4-134c-4f1d-8fc5-15e530dd975c` (visited on 06/14/2022).

[93] *Most electricity are produced in Norrland while most electricity are used in western Sweden*, Feb. 2018. [Online]. Available: `https://www.scb.se/en/finding- statistics / statistics - by - subject - area / energy / energy - balances / local - and - regional - energy - statistics / pong / statistical - news / local-and-regional-energy-statistics/` (visited on 06/14/2022).

[94] "SWEDEN - TOWARDS 100% RENEWABLE ENERGY," [Online]. Available: `https://www.andritz.com/hydro-en/hydronews/hn-europe/sweden#:~: text=There%20are%20about%2016%2C301%20MW,%2C%20Indals%C3%A4lv% 2C%20Ume%C3%A4lv%20and%20%C3%85ngerman%C3%A4lv..`

[95] *Variable Cost Concepts for Power Generation*. [Online]. Available: `https://www. e - education . psu . edu / ebf483 / node / 584# : ~ : text = The % 20simplest % 20model % 20for % 20variable , is % 20dominated % 20by % 20fuel % 20costs.` (visited on 05/24/2022).

[96] "Renewable Power Generation Costs 2020," en, p. 180, 2020. [Online]. Available: `https : / / www . irena . org / publications / 2021 / Jun / Renewable - Power - Costs-in-2020` (visited on 05/24/2022).

[97] *Cost Assumptions*. [Online]. Available: `https://pypsa-eur.readthedocs.io/en/latest/costs.html` (visited on 05/24/2022).

[98] O. Tang, J. Rehme, P. Cerin, and D. Huisingh, "Hydrogen production in the Swedish power sector: Considering operational volatilities and long-term uncertainties," en, *Energy Policy*, vol. 148, p. 111 990, Jan. 2021, ISSN: 03014215. DOI: `10.1016/j.enpol.2020.111990`. [Online]. Available: `https://linkinghub.elsevier.com/retrieve/pii/S0301421520307011` (visited on 05/24/2022).

[99] *Granted projects within Regional Electrification Pilots*.

[100] *Major expansion of electricity and hydrogen gas stations for goods following a decision from the Energy Agency*, Aug. 2022. [Online]. Available: `https://www.voltimum.se/articles/branschnyheter/stor-utbyggnad-av-el-och`.